



International Institute for  
Applied Systems Analysis  
Schlossplatz 1  
A-2361 Laxenburg, Austria

Tel: +43 2236 807 342  
Fax: +43 2236 71313  
E-mail: [publications@iiasa.ac.at](mailto:publications@iiasa.ac.at)  
Web: [www.iiasa.ac.at](http://www.iiasa.ac.at)

---

**Interim Report**

**IR-12-043**

**Evolutionary-branching lines and areas in bivariate trait spaces**

Hiroshi C. Ito

Ulf Dieckmann ([dieckmann@iiasa.ac.at](mailto:dieckmann@iiasa.ac.at))

---

**Approved by**

Pavel Kabat

Director General and Chief Executive Officer

February 2015

---

*Interim Reports* on work of the International Institute for Applied Systems Analysis receive only limited review. Views or opinions expressed herein do not necessarily represent those of the Institute, its National Member Organizations, or other organizations supporting the work.

# 1 **Evolutionary-branching lines and areas in bivariate trait spaces**

2 Hiroshi C. Ito<sup>1</sup> and Ulf Dieckmann<sup>1</sup>

3 <sup>1</sup>*Evolution and Ecology Program, International Institute for Applied Systems Analysis,*  
4 *Schlossplatz 1, A-2361 Laxenburg, Austria*

5 E-mail addresses: H. C. Ito, [hiroshibeetle@gmail.com](mailto:hiroshibeetle@gmail.com); U. Dieckmann, [dieckmann@iiasa.ac.at](mailto:dieckmann@iiasa.ac.at)

## 6 **ABSTRACT**

7 **Aims:** Evolutionary branching is a process of evolutionary diversification induced by fre-  
8 quency-dependent ecological interaction. Here we show how to predict the occurrence of evo-  
9 lutionary branching in bivariate traits when populations are evolving directionally.

10 **Methods:** Following adaptive dynamics theory, we assume low mutation rates and small  
11 mutational step sizes. On this basis, we generalize conditions for evolutionary-branching  
12 points to conditions for evolutionary-branching lines and areas, which delineate regions of  
13 trait space in which evolutionary branching can be expected despite populations still evolving  
14 directionally along these lines and within these areas. To assess the quality of predictions pro-  
15 vided by our new conditions for evolutionary branching lines and areas, we analyse three eco-  
16 evolutionary models with bivariate trait spaces, comparing the predicted evolutionary-  
17 branching lines and areas with actual occurrences of evolutionary branching in numerically  
18 calculated evolutionary dynamics. In the three examples, a phenotype's fitness is affected by  
19 frequency-dependent resource competition and/or predator–prey interaction.

20 **Conclusions:** In the limit of infinitesimal mutational step sizes, evolutionary branching in  
21 bivariate trait spaces can occur only at evolutionary-branching points, i.e., where the evolving  
22 population experiences disruptive selection in the absence of any directional selection. In con-  
23 trast, when mutational step sizes are finite, evolutionary branching can occur also along evo-  
24 lutionary-branching lines, i.e., where disruptive selection orthogonal to these lines is suffi-  
25 ciently strong relative to directional selection along them. Moreover, such evolutionary-  
26 branching lines are embedded in evolutionary-branching areas, which delineate all bivariate  
27 trait combinations for which evolutionary branching can occur when mutation rates are low,

1 while mutational step sizes are finite. Our analyses show that evolutionary-branching lines  
2 and areas are good indicators of evolutionary branching in directionally evolving populations.  
3 We also demonstrate that not all evolutionary-branching lines and areas contain evolutionary-  
4 branching points, so evolutionary branching is possible even in trait spaces that contain no  
5 evolutionary-branching point at all.

## 6 **INTRODUCTION**

7 Evolutionary branching is a process of evolutionary diversification induced by ecological in-  
8 teraction (Metz *et al.*, 1992; Geritz *et al.*, 1997, 1998; Dieckmann *et al.*, 2004), which can  
9 occur through all fundamental types of ecological interaction, including competition, preda-  
10 tor-prey interaction, and mutualism (Doebeli and Dieckmann, 2000; Dieckmann *et al.*, 2007).  
11 Therefore, evolutionary branching may be an important mechanism underlying the sympatric  
12 or parapatric speciation of sexual populations driven by frequency-dependent selection pres-  
13 sures (e.g., Doebeli, 1996; Dieckmann and Doebeli, 1999; Kisdi and Geritz, 1999; Doebeli  
14 and Dieckmann, 2003; Dieckmann *et al.*, 2004; Claessen *et al.*, 2008; Durinx and Van Door-  
15 en, 2009; Heinz *et al.*, 2009; Payne *et al.*, 2011).

16 In asexual populations with rare and small mutational steps, evolutionary branching oc-  
17 curs through trait-substitution sequences caused by the sequential invasion of successful mu-  
18 tants. In univariate trait spaces, a necessary and sufficient condition for evolutionary branch-  
19 ing is the existence of a convergence stable trait value, called an evolutionary-branching  
20 point, at which directional selection is absent and the remaining selection is locally disruptive  
21 (Metz *et al.*, 1992; Geritz *et al.*, 1997).

22 Real populations, however, have undergone, and are usually undergoing, evolution in  
23 many quantitative traits, with large variation in their evolutionary speeds (e.g., Hendry and  
24 Kinnison, 1999; Kinnison and Hendry, 2001). Such speed differences among traits may be  
25 due to smaller mutation rates and/or magnitudes in some traits than in others, and will also  
26 arise when fitness is less sensitive to some traits than to others.

27 Only a few previous studies have analytically investigated evolutionary branching in mul-  
28 tivariate trait spaces (Ackermann and Doebeli, 2004; Egas *et al.*, 2005; Leimar, 2005; Ravi-

1 gné *et al.*, 2009). Those studies assumed that all considered traits evolve at comparable  
2 speeds, and analyzed possibilities of evolutionary branching by examining the existence of  
3 evolutionary-branching points having the following four properties: evolutionary singularity  
4 (no directional selection), convergence stability (local evolutionary attractor for monomorphic  
5 evolution), evolutionary instability (locally disruptive selection), and mutual invasibility (lo-  
6 cal coexistence of dimorphic trait values). All of these studies have therefore considered the  
7 vanishing of directional selection as a prerequisite for evolutionary branching.

8 On the other hand, Ito and Dieckmann (2007) have numerically shown that, when muta-  
9 tional step sizes are not infinitesimal, evolutionary branching can occur even in directionally  
10 evolving populations, as long as directional evolution is sufficiently slow. This implies that  
11 trait spaces may contain evolutionary-branching lines that attract monomorphic evolution and  
12 then induce evolutionary branching while populations are directionally evolving along them.  
13 Furthermore, Ito and Dieckmann (submitted) derived sufficient conditions for the existence of  
14 such evolutionary-branching lines, by focusing on trait-substitution sequences formed by in-  
15 vasions each of which possesses maximum likelihood, called maximum-likelihood invasion  
16 paths (MLIPs).

17 In this study, we heuristically extend the derived sufficient conditions for evolutionary-  
18 branching lines to sufficient conditions for evolutionary-branching areas, and apply these two  
19 sets of conditions to three eco-evolutionary models with bivariate trait spaces. Our study is  
20 structured as follows. The next section explains conditions for evolutionary-branching lines  
21 and extends those to evolutionary-branching areas. In the first example, we apply the two sets  
22 of conditions to a resource-competition model with two evolving niche positions. In the se-  
23 cond example, we show their application to another resource-competition model with evolv-  
24 ing niche position and niche width. In the third example, a predator-prey model with two  
25 evolving niche positions is analyzed. The last section discusses how our conditions improve  
26 understanding of evolutionary branching in multivariate trait spaces.

# 1 CONDITIONS FOR EVOLUTIONARY-BRANCHING LINES AND AREAS

2 In this section, we review and explain the sufficient conditions for evolutionary-branching  
3 lines (Ito and Dieckmann, submitted) and extend them to evolutionary-branching areas. We  
4 consider bivariate trait spaces spanned by two scalar traits  $X$  and  $Y$ , denoted by  
5  $\mathbf{S} = (X, Y)^T$  (where  $T$  denotes transposition). The conditions for evolutionary-branching  
6 lines and areas are analyzed by introducing a locally normalized coordinate system  
7  $\mathbf{s} = (x, y)^T$  at each point of the original coordinate system  $\mathbf{S} = (X, Y)^T$ . Throughout this pa-  
8 per, all model definitions, figures, and verbal discussions of the models are presented in terms  
9 of the original coordinate systems, while the analytic conditions, e.g., in Eqs. (1-3), are pre-  
10 sented using the locally normalized coordinate systems.

## 11 Local normalization of invasion-fitness function

12 We consider an asexual monomorphic population in an arbitrary bivariate trait space  
13  $\mathbf{S} = (X, Y)^T$ . Throughout this study, we assume low mutation rates and small mutational step  
14 sizes. Under the former assumption, the population is almost always close to population-  
15 dynamical equilibrium when a mutant emerges. It can then also be shown that, in the absence  
16 of population-dynamical bifurcations and when mutational step sizes are not only small, but  
17 infinitesimal, the population remains monomorphic in the course of directional evolution  
18 (Geritz *et al.*, 2002): under these conditions, a mutant phenotype  $\mathbf{S}'$  can invade and replace a  
19 resident phenotype  $\mathbf{S}$  if its invasion fitness is positive, resulting in what is called a trait sub-  
20 stitution.

21 The invasion fitness of  $\mathbf{S}'$  under  $\mathbf{S}$ , denoted by  $F(\mathbf{S}'; \mathbf{S})$ , is defined as the exponential  
22 growth rate of a small population of phenotypes  $\mathbf{S}'$  in the environment created by a mono-  
23 morphic population of phenotypes  $\mathbf{S}$  at its population-dynamical equilibrium (Metz *et al.*,  
24 1992). The invasion-fitness function  $F$  can be interpreted as a fitness landscape in  $\mathbf{S}'$ ,  
25 whose shape depends on  $\mathbf{S}$ . For small mutational step sizes, repeated invasion and replace-  
26 ment of  $\mathbf{S}$  by  $\mathbf{S}'$  in the direction of the fitness gradient  $\partial F(\mathbf{S}'; \mathbf{S}) / \partial \mathbf{S}'|_{\mathbf{S}'=\mathbf{S}}$  brings about a  
27 trait-substitution sequence, resulting in gradual directional evolution (Metz *et al.*, 1992;  
28 Dieckmann *et al.*, 1995; Dieckmann and Law, 1996; Geritz *et al.*, 2002).

1 When a mutant emerges, which occurs with probability  $\mu$  per birth, we assume that its  
 2 phenotype  $\mathbf{S}'$  follows a mutation probability distribution  $M(\mathbf{S}' - \mathbf{S})$  given by a bivariate  
 3 normal distribution with mean  $\mathbf{S}$  (Appendix A). The distribution of mutational step sizes  
 4 may depend on the direction of  $\mathbf{S}' - \mathbf{S}$ , according to the variance-covariance matrix of  $M$ .

5 In this trait space, evolutionary dynamics depend on the invasion-fitness function  $F$  and  
 6 the mutation probability distribution  $M$ . To describe this dependence, we consider a mono-  
 7 morphic population of phenotypes  $\mathbf{S}_0$ , and to simplify notation and analysis, we introduce a  
 8 locally normalized coordinate system  $\mathbf{s} = (x, y)^T$  having its origin at  $\mathbf{S}_0$ . This local coordi-  
 9 nate system is scaled so that the standard deviation of mutational step sizes, equaling the root-  
 10 mean-square mutational step size, is  $\sigma$  in all directions. The asymmetry (non-isotropy) of  
 11 mutations is thus absorbed into the invasion-fitness function, resulting in a normalized inva-  
 12 sion-fitness function denoted by  $f(\mathbf{s}'; \mathbf{s})$ .

13 The local shape of  $f$  around the origin  $\mathbf{s} = 0$  ( $\mathbf{S} = \mathbf{S}_0$ ) can be approximated by a Taylor  
 14 expansion in  $\mathbf{s}$  and  $\delta\mathbf{s} = (\delta x, \delta y)^T = \mathbf{s}' - \mathbf{s}$  up to second order,

$$15 \quad f(\mathbf{s}'; \mathbf{s}) = \mathbf{G} \delta\mathbf{s} + \frac{1}{2} \mathbf{s}^T \mathbf{C} \delta\mathbf{s} + \frac{1}{2} \delta\mathbf{s}^T \mathbf{D} \delta\mathbf{s}, \quad (1)$$

16 with the row vector  $\mathbf{G} = (G_x, G_y)$  and the matrices  $\mathbf{C} = ((C_{xx}, C_{xy}), (C_{yx}, C_{yy}))^T$  and  
 17  $\mathbf{D} = ((D_{xx}, 0), (0, D_{yy}))^T$ . The other possible terms in this expansion, proportional to  $\mathbf{s}$  and  
 18  $\mathbf{s}^T \mathbf{s}$ , vanish because  $f(\mathbf{s}; \mathbf{s}) = 0$  holds at population-dynamical equilibrium for arbitrary  $\mathbf{s}$ .  
 19 The vector  $\mathbf{G} = \partial f(\mathbf{s}'; \mathbf{s}) / \partial \mathbf{s}' |_{\mathbf{s}' = \mathbf{s} = 0}$  is the fitness gradient: it measures the steepest ascent of  
 20  $f$  with respect to  $\mathbf{s}'$ , and thus describes directional selection for a population at the origin.  
 21 The matrix  $\mathbf{C} = \partial^2 f(\mathbf{s}'; \mathbf{s}) / (\partial \mathbf{s}' \partial \mathbf{s}) |_{\mathbf{s}' = \mathbf{s} = 0}$  measures how directional selection changes as the  
 22 population deviates from the origin, and thus describes evolutionary convergence to, and/or  
 23 divergence from, the origin. The symmetric matrix  $\mathbf{D} = \partial^2 f(\mathbf{s}'; \mathbf{s}) / \partial \mathbf{s}'^2 |_{\mathbf{s}' = \mathbf{s} = 0}$  measures the  
 24 second derivative, or curvature, of  $f$  with respect to  $\mathbf{s}'$ , and thus describes disruptive  
 25 and/or stabilizing selection at the origin. The local coordinate system  $\mathbf{s} = (x, y)^T$  can always  
 26 be chosen, by adjusting the directions of the  $x$ - and  $y$ -axes, so that  $\mathbf{D}$  is diagonal and  
 27  $D_{xx} \geq D_{yy}$ . Thus, when disruptive selection exists, it has maximum strength along the  $x$ -axis.  
 28 Notice that  $\mathbf{G}$ ,  $\mathbf{C}$ , and  $\mathbf{D}$  are functions of the base point  $\mathbf{S}_0$ .

## 1 **Conditions for evolutionary-branching lines**

2 A typical situation allowing evolutionary branching of a directionally evolving population  
3 occurs when mutational step sizes are significantly smaller in one trait direction than in the  
4 other, when considered in the original coordinate system  $\mathbf{S} = (X, Y)^T$ . In this case, the popu-  
5 lation quickly evolves in the direction of the larger step size until it no longer experiences  
6 directional selection in that direction, while it continues slow directional evolution in the other  
7 direction. Then, if the population experiences sufficiently strong disruptive selection along the  
8 fast direction compared to directional selection along the slow direction, evolutionary branch-  
9 ing may occur.

10 This conclusion has been demonstrated by Ito and Dieckmann (submitted), who analyti-  
11 cally derived sufficient conditions for the existence of an evolutionary-branching line passing  
12 through  $\mathbf{S}_0$  (by focusing on trait-substitution sequences formed by invasions each of which  
13 possesses maximum likelihood, so-called maximum-likelihood invasion paths or MLIPs). In  
14 the locally normalized coordinate system  $\mathbf{s} = (x, y)^T$  at  $\mathbf{S}_0$ , these conditions come in three  
15 parts,

$$16 \quad G_x = 0, \quad (2a)$$

$$17 \quad C_{xx} < 0, \quad (2b)$$

18 and

$$19 \quad \frac{\sigma D_{xx}}{|G_y|} > \sqrt{2}. \quad (2c)$$

20 While Eqs. (2) were analytically derived assuming that  $C_{yy}$ ,  $C_{xy}$ ,  $C_{yx}$ , and  $D_{yy}$  are negli-  
21 gible, it is expected that these conditions work well even when this simplifying assumption is  
22 relaxed, as explained by Ito and Dieckmann (submitted). Eq. (2a) ensures the absence of di-  
23 rectional selection in  $x$ . Eqs. (2a) and (2b) ensure convergence, through directional evolu-  
24 tion, of monomorphic populations to the evolutionary-branching line  $x = 0$ . After sufficient  
25 convergence, inequality (2c) ensures evolutionary branching, which according this is inequali-  
26 ty occurs when disruptive selection  $D_{xx}$  orthogonal to  $x = 0$  is sufficiently strong com-

1   pared to directional selection  $G_y$  along  $x=0$ . The smaller the standard deviation  $\sigma$  of  
2   mutation step sizes, the stronger disruptive selection  $D_{xx}$  must be relative to directional se-  
3   lection  $G_y$  for evolutionary branching to occur.

4       Notice that as  $|G_y| \rightarrow 0$ , inequality (2c) converges to  $D_{xx} > 0$ , so that in this limiting case  
5   conditions for evolutionary-branching lines in bivariate trait spaces become identical to condi-  
6   tions for evolutionary-branching points in univariate trait spaces (Metz *et al.*, 1992; Geritz *et*  
7   *al.*, 1997). Similarly, when  $\sigma \rightarrow 0$ , inequality (2c) requires  $G_y = 0$  and  $D_{xx} > 0$ , which  
8   shows that for infinitesimal mutation steps evolutionary branching can occur only in the ab-  
9   sence of all directional selection.

10       By examining conditions (2) for all phenotypes  $S_0$  in a considered trait space, and by  
11   then connecting those phenotypes that fulfill these conditions, evolutionary-branching lines  
12   are identified. According to the derivation of conditions (2), it is ensured that any MLIP start-  
13   ing from a monomorphic population of phenotypes sufficiently close to an evolutionary-  
14   branching line immediately converges to that line and then brings about evolutionary branch-  
15   ing (Ito and Dieckmann, submitted). Also trait-substitution sequences that are not MLIPs then  
16   show a very high likelihood of evolutionary branching (Ito and Dieckmann, submitted).

## 17   **Conditions for evolutionary branching areas**

18   We now extend conditions for evolutionary-branching lines to evolutionary-branching areas.  
19   As explained below, two special cases are analytically tractable; the extended conditions are  
20   then obtained heuristically by treating intermediate cases through interpolation.

21       While conditions (2) were derived as sufficient conditions for evolutionary branching, it is  
22   likely that in particular the equality condition (2a) is too strict, as evolutionary branching does  
23   not require  $G_x = 0$ , but only that  $|G_x|$  be sufficiently small. But how small is small enough?  
24   To answer this question, we have to extend inequality (2c) to phenotypes that are not on an  
25   evolutionary-branching line. For such phenotypes, the orthogonality between the directions of  
26   directional selection and of maximum disruptive selection, which strictly holds on evolution-  
27   ary-branching lines and is only negligibly disturbed in their immediate vicinity (Ito and  
28   Dieckmann, submitted), is increasingly relaxed the farther these phenotypes are displaced

1 from such lines. Fortunately, the emergence of a protected dimorphism along MLIPs, which  
 2 underlies inequality (2c), can be studied analytically also for the opposite case, in which the  
 3 direction of directional selection is parallel to that of maximum disruptive selection (Appen-  
 4 dix B). By interpolating between these two special cases, we can generalize inequality (2c) to  
 5 intermediate cases, in which directional selection is neither orthogonal nor parallel to disrup-  
 6 tive selection,

$$7 \quad \frac{\sigma D_{xx}}{|\tilde{\mathbf{G}}|} > \sqrt{2} \quad \text{with} \quad \tilde{\mathbf{G}} = (\sqrt{2}G_x, G_y). \quad (3a)$$

8 The factor  $\sqrt{2}$  in the definition of  $\tilde{\mathbf{G}}$  means that directional selection in  $x$  hinders evolu-  
 9 tionary branching in  $y$  slightly more, but this factor of  $\sqrt{2}$ , than directional selection in  
 10  $y$ .

11 By combining inequalities (2b) and (3a), we obtain conditions for evolutionary-branching  
 12 areas, as it was Eq. (2a) that limits conditions (2) to being fulfilled just along lines. Evolution-  
 13 ary-branching areas always surround evolutionary-branching lines when such lines exist, but  
 14 additionally comprise phenotypes for which, in violation of Eq. (2a), directional evolution has  
 15 not yet converged to those lines.

16 Since the conditions for evolutionary-branching lines and areas are derived as sufficient  
 17 conditions (for the emergence of a protected dimorphism along MLIPs), the length of these  
 18 lines and the size of these areas are expected to be conservative. Thus, adjusting the threshold  
 19 value in Eq. (3a) may be useful for explaining observed patterns of evolutionary branching.  
 20 For this purpose, we introduce the parameter  $\rho$  with  $0 < \rho \leq 1$  into Eq. (3a), which gives

$$21 \quad \frac{\sigma D_{xx}}{|\tilde{\mathbf{G}}|} > \sqrt{2}\rho. \quad (3b)$$

22 Below, we illustrate the effect of  $\rho$  by considering  $\rho = 0.2$ . We call the combination of  
 23 inequalities (2b) and (3b) the 20%-threshold condition for evolutionary-branching areas, and  
 24 we refer to areas fulfilling this condition as 20%-threshold areas. For specific procedures that  
 25 are useful for the practical identification of evolutionary-branching lines and areas, see Ap-  
 26 pendix C.

## 1 **Sizes and shapes of evolutionary-branching lines and areas**

2 As a simple example, we now briefly explain how an evolutionary-branching line and area are  
3 identified around an evolutionary-branching point located at the origin of a trait space  
4  $\mathbf{S} = (X, Y)^T$ . See Appendix E for details.

5 We assume that the strengths of convergence stability of the origin along the  $X$ - and  $Y$ -  
6 axes are given by the two negative scalars  $C_{XX}$  and  $C_{YY}$ , respectively. We also assume that  
7 the maximum disruptive selection in this original coordinate system occurs along the  $X$ -  
8 axis, quantified by the positive scalar  $D_{XX}$  (i.e.,  $D_{XX} > D_{YY}$ ). In addition, we denote the  
9 standard deviations of mutational step sizes along the  $X$ - and  $Y$ -axes by  $\sigma_X$  and  $\sigma_Y$ ,  
10 respectively. We assume that these steps have no mutational correlation,  $\sigma_{XY} = 0$ , and that  
11 they are largest along the  $X$ -axis,  $\sigma_X > \sigma_Y$ . In this case, for each phenotype  $\mathbf{S}_0 = (X_0, Y_0)^T$   
12 close to the origin, local normalization provides the matrices  $\mathbf{G}$ ,  $\mathbf{C}$ , and  $\mathbf{D}$  in Eq. (1),  
13 without the need for any coordinate rotation; i.e., the  $x$ -axis is parallel to the  $X$ -axis.

14 By examining Eqs. (2) and Eq. (3a) based on the derived matrices  $\mathbf{G}$ ,  $\mathbf{C}$ , and  $\mathbf{D}$ , we  
15 find, expressed in the original coordinate system, an evolutionary-branching line as a straight  
16 line segment,

$$17 \quad X_0 = 0 \quad \text{and} \quad |Y_0| < r_Y, \quad (4)$$

18 and an evolutionary-branching area as a filled ellipse,

$$19 \quad \frac{X_0^2}{r_X^2} + \frac{Y_0^2}{r_Y^2} < 1, \quad (5a)$$

20 with a radius of

$$21 \quad r_X = \frac{\sigma_X D_{XX}}{2|C_{XX}|} \quad (5b)$$

22 along the  $X$ -axis and a radius of

$$23 \quad r_Y = \frac{\sigma_X D_{XX}}{\sqrt{2}|C_{YY}|} \cdot \frac{\sigma_X}{\sigma_Y} \quad (5c)$$

24 along the  $Y$ -axis.

1 Notice that the length of the evolutionary-branching line coincides with the radius of the  
 2 evolutionary-branching area along the  $Y$ -axis. According to Eqs. (5), if the difference in  
 3 magnitude between  $\sigma_X$  and  $\sigma_Y$  is kept small, large mutational step sizes and/or strong dis-  
 4 ruptive selection pressures result in large evolutionary-branching areas. On the other hand,  
 5 according to Eq. (5c), when  $\sigma_Y$  is small compared to  $\sigma_X$ , the shape of the evolutionary-  
 6 branching area is elongated along the  $Y$ -axis, even if  $\sigma_X$  is small. Since infinitesimally  
 7 small  $\sigma_Y$  make this situation identical to that of a univariate trait space comprising trait  $X$   
 8 alone, Eq. (5b) may work also for predicting one-dimensional evolutionary-branching areas  
 9 surrounding evolutionary-branching points in univariate trait spaces.

## 10 **FIRST EXAMPLE: RESOURCE-COMPETITION MODEL WITH** 11 **EVOLVING NICHE POSITIONS**

12 In this section, we apply our conditions for evolutionary-branching lines and areas to a model  
 13 of niche evolution under intraspecific resource competition (Vukics and Meszena, 2003; Ito  
 14 and Dieckmann, 2007), which is a bivariate extension of seminal models by MacArthur and  
 15 Levins (MacArthur and Levins, 1967; MacArthur, 1972) and Roughgarden (1974, 1976). This  
 16 example illustrates how an evolutionary-branching point transforms into an evolutionary-  
 17 branching line when differences in mutational step sizes among two trait directions become  
 18 sufficiently large.

### 19 **Model description**

20 We consider a bivariate trait space  $\mathbf{S} = (X, Y)^T$ , with  $X$  and  $Y$  denoting evolving traits  
 21 that determine a phenotype's bivariate niche position. The growth rate of phenotype  $\mathbf{S}_i$  is  
 22 given by

$$23 \quad \frac{dn_i}{dt} = n_i \left[ 1 - \sum_{j=1}^L \alpha(\mathbf{S}_i - \mathbf{S}_j) n_j / K(\mathbf{S}_i) \right], \quad (6a)$$

24 where  $L$  is the number of resident phenotypes. The carrying capacity  $K(\mathbf{S}_i)$  of phenotype  
 25  $\mathbf{S}_i$  is given by an isotropic bivariate normal distribution,

$$26 \quad K(\mathbf{S}_i) = K_0 \exp\left(-\frac{1}{2} |\mathbf{S}_i|^2 / \sigma_K^2\right), \quad (6b)$$

1 with maximum  $K_0$ , mean  $(0,0)^T$ , and standard deviation  $\sigma_K$ . The strength  $\alpha(\mathbf{S}_i - \mathbf{S}_j)$  of  
 2 competition between phenotype  $\mathbf{S}_i$  and phenotype  $\mathbf{S}_j$  is also given by an isotropic bivari-  
 3 ate normal distribution,

$$4 \quad \alpha(\mathbf{S}_i - \mathbf{S}_j) = \exp(-\frac{1}{2} |\mathbf{S}_i - \mathbf{S}_j|^2 / \sigma_\alpha^2), \quad (6c)$$

5 with maximum 1, mean  $(0,0)^T$ , and standard deviation  $\sigma_\alpha$ , so the strength of competition is  
 6 maximal between identical phenotypes  $\mathbf{S}_i = \mathbf{S}_j$  and monotonically declines with phenotypic  
 7 distance  $|\mathbf{S}_i - \mathbf{S}_j|$ .

8 In this model, carrying capacity is maximal at the origin  $\mathbf{S} = (0,0)^T$ , which therefore  
 9 serves as a unique convergence stable phenotype, or global evolutionary attractor, to which  
 10 monomorphic populations converge through directional evolution. After sufficient conver-  
 11 gence, if the width  $\sigma_\alpha$  of the competition kernel is narrower than the width  $\sigma_K$  of the car-  
 12 rying-capacity distribution, the resultant fitness landscape has a minimum at the origin, which  
 13 induces evolutionary branching of the evolving population. Thus,  $\sigma_\alpha < \sigma_K$  is the condition  
 14 for existence of an evolutionary-branching point in this model (Vukics and Meszena, 2003),  
 15 in analogy with the univariate case (Roughgarden, 1972; Dieckmann and Doebeli, 1999).

16 As for the mutation probability distribution, we define its variance-covariance matrix so  
 17 that the standard deviation of mutational step sizes has a maximum  $\sigma_1$  in the direction of  
 18  $\mathbf{e}_1 = (-1,1)^T$  and a minimum  $\sigma_2$  in the direction of  $\mathbf{e}_2 = (1,1)^T$ .

19 Notice that fitness in this model is rotationally symmetric in terms of the traits  $X$  and  
 20  $Y$  (i.e., rotating all phenotypes around the origin does not change their fitnesses). Thus, a  
 21 sensitivity difference of the normalized invasion-fitness function can arise only from the con-  
 22 sidered difference in mutational step sizes along the two directions  $\mathbf{e}_1$  and  $\mathbf{e}_2$ .

## 23 **Predicted evolutionary-branching lines and areas**

24 When mutational step sizes are isotropic, the predicted evolutionary-branching area forms a  
 25 circle around the evolutionary-branching point, and contains no evolutionary-branching line  
 26 (not shown). In this case, occurrences of evolutionary branching are explained well by the  
 27 evolutionary-branching point alone. Because of the rotational symmetry in fitness, there is no

1 restriction on the direction of evolutionary branching, so that evolutionary diversification can  
2 occur in any direction (Vukis and Meszéna, 2003). Although this case is reminiscent of that of  
3 a univariate trait defined by the distance from the evolutionary-branching point, these two  
4 cases are not equivalent: this is because in the univariate case disruptive selection and direc-  
5 tional selection are always parallel, while in the isotropic bivariate case disruptive selection  
6 may be orthogonal to directional selection.

7 Figure 2a shows that when the difference in mutational step size between directions  $\mathbf{e}_1$   
8 and  $\mathbf{e}_2$  is substantial (e.g.,  $\sigma_1 / \sigma_2 = 3$ ), the evolutionary-branching line and area expand in  
9 the direction of the smaller mutational step size ( $\mathbf{e}_2$  in this case). In addition, the direction of  
10 expected evolutionary diversification is getting the more restricted to  $\mathbf{e}_1$  the larger this dif-  
11 ference becomes. [If  $\mathbf{e}_1$  and  $\mathbf{e}_2$  were pointing along the  $Y$ - and  $X$ -axes, respectively, the  
12 situation would correspond to Eqs. (4) and (5).] In Fig. 2a, the short purple line and the small  
13 purple area (both situated within the light-purple area) depict the predicted evolutionary-  
14 branching line and area, with their colors indicating the predicted direction of diversification.  
15 Because of the difference in mutational step sizes between the two directions, it is expected  
16 that a monomorphic population quickly converges to the line  $Y = X$  (gray arrows) and then  
17 slowly converges to the evolutionary-branching area. Evolutionary branching is expected to  
18 occur at the latest once evolution has reached this area, because our conditions for an evolu-  
19 tionary-branching area are derived as sufficient conditions and imply the possibility of an  
20 immediate start of evolutionary branching of a monomorphic population in its inside. Accord-  
21 ingly, evolutionary branching may occur well before the population has reached the evolu-  
22 tionary-branching area. The light-purple area shows the corresponding 20%-threshold area,  
23 comprising all phenotypes that fulfill the 20%-threshold condition for evolutionary-branching  
24 areas. By definition, an evolutionary-branching area is always included in the corresponding  
25 20%-threshold area. The larger the difference in mutational step sizes between the two direc-  
26 tions, the longer the evolutionary-branching line and the more elongated the evolutionary-  
27 branching area, as predicted by Eq. (5c)

## 1 **Comparison with actual evolutionary dynamics**

2 Figure 2b shows occurrences of evolutionary branching in numerically calculated evolution-  
3 ary dynamics starting from monomorphic populations with phenotypes randomly chosen  
4 across the shown trait space: each occurrence is depicted by an open triangle whose color in-  
5 dicates the direction of that particular evolutionary branching. The evolutionary dynamics are  
6 numerically calculated as trait-substitution sequences according to the oligomorphic stochas-  
7 tic model of adaptive dynamics theory (Ito and Dieckmann, 2007; for the sake of computa-  
8 tional efficiency, phenotypes with densities below a threshold  $\varepsilon_e$  are removed, with the val-  
9 ue of  $\varepsilon_e$  being immaterial as long as it is small enough). The relative shape of the cluster of  
10 occurrences is characterized well by the evolutionary-branching area, or here almost equiva-  
11 lently, by the evolutionary-branching line. Moreover, the absolute shape, and hence the size,  
12 of this cluster is well matched by that of the 20%-threshold area. The fact that the colors of  
13 the triangles in Fig. 2b are very similar to that of the evolutionary-branching area in Fig. 2a  
14 demonstrates that also the predicted and actual directions of diversification are in good  
15 agreement.

16 Figure 2b shows two evolutionary trajectories, depicted as dark-yellow and green curves,  
17 respectively. These illustrate that monomorphic populations initially converge to the line  
18  $Y = X$ . Then, if the population is already inside the evolutionary-branching area, it immedi-  
19 ately undergoes evolutionary branching, as expected (green curves in Fig. 2b and Fig. 2d). In  
20 contrast, if the population still remains outside the evolutionary-branching area, it continues  
21 directional evolution along the line  $Y = X$  towards the evolutionary-branching area. As ex-  
22 pected, evolutionary branching may occur before the population has reached the evolution-  
23 ary-branching area (dark-yellow curves in Fig. 2b and Fig. 2c).

24 In summary, this first example shows how differences in mutational step sizes among trait  
25 directions can transform an evolutionary-branching point into an evolutionary-branching line  
26 or an elongated evolutionary-branching area.

## 1 SECOND EXAMPLE: RESOURCE-COMPETITION MODEL WITH EVOLV- 2 ING NICHE POSITION AND NICHE WIDTH

3 In this section, based on another type of resource-competition model, we show that an evolu-  
4 tionary-branching area can exist without containing any evolutionary-branching point.

### 5 Model description

6 For phenotypes  $\mathbf{S} = (X, Y)^T$  in our second example, the trait  $X$  still determines the pheno-  
7 type's niche position, like in the first model, whereas the trait  $Y$  now determines the pheno-  
8 type's niche width, differently from the first model. This niche width can be interpreted in  
9 terms of the variety of resource types utilized by the phenotype. We assume a constant and  
10 unimodal distribution  $R(z)$  of univariate resource types  $z$ , given by a normal distribution,

$$11 \quad R(z) = R_0 N(z, m_R, \sigma_R^2), \quad (7a)$$

12 with  $N(z, m, \sigma^2) = \exp(-\frac{1}{2}(z-m)^2 / \sigma^2) / (\sqrt{2\pi}\sigma)$ . Here,  $R_0$ ,  $m_R$ , and  $\sigma_R$  denote the re-  
13 source distribution's integral, mean, and standard deviation. Similarly, the niche of a pheno-  
14 type  $\mathbf{S}_i$  is specified by a normal distribution across resource types  $z$ , with mean  $X_i$  (niche  
15 position) and standard deviation  $Y_i$  (niche width),

$$16 \quad c(z, \mathbf{S}_i) = N(z, X_i, Y_i^2). \quad (7b)$$

17 The rate of potential resource gain of phenotype  $\mathbf{S}_i$  per unit of its biomass is given by the  
18 overlap integral, over all resource types  $z$ , of its niche  $c(z, \mathbf{S}_i)$  and the resource distribution  
19  $R(z)$ . The corresponding rate of actual resource gain  $g(\mathbf{S}_i)$  incorporates a functional re-  
20 sponse, derived in Appendix D as an extension of the Beddington-DeAngelis-type functional  
21 response (Beddington, 1975; DeAngelis *et al.*, 1975), known to ensure both saturation of con-  
22 sumption and interference competition among consumers. On this basis, the growth rate of  
23 phenotype  $\mathbf{S}_i$  is given by

$$24 \quad \frac{dn_i}{dt} = n_i[\lambda g(\mathbf{S}_i) - d(Y_i)], \quad (7c)$$

1 where the constant  $\lambda$  measures trophic efficiency (i.e., biomass production per biomass  
2 gain) and  $d(Y_i)$  is the biomass loss of phenotype  $S_i$  due to basic metabolism and natural  
3 death, with the dependence on  $Y_i$  reflecting costs of specialization or generalization.

4 As for the mutation distribution, we use a simple bivariate normal distribution in which  
5 the standard deviation of mutational step sizes has its maximum  $\sigma_X$  in the  $X$ -direction and  
6 its minimum  $\sigma_Y$  in the  $Y$ -direction. See Appendix E for further model details.

## 7 **Predicted evolutionary-branching lines and areas**

8 Figure 3a shows the directional evolution (gray arrows) of monomorphic populations and the  
9 predicted evolutionary-branching lines and areas, as in Fig. 2a, for the case that specialization  
10 (narrow niche width) is costly. This shows that niche position and niche width directionally  
11 evolve so as to become more similar, respectively, to the center and width of the resource  
12 distribution. We find two kinds of evolutionary-branching areas. As indicated by the color  
13 coding, the small blue evolutionary-branching area around the center of the shown trait space  
14 induces evolutionary branching in the direction of niche width. This evolutionary-branching  
15 area contains an evolutionary-branching point at its center and is attracting any monomorphic  
16 population in the trait space. In this regard, this evolutionary-branching area is similar to that  
17 in the first model. In contrast, the red evolutionary-branching area around the bottom of the  
18 shown trait space contains no evolutionary-branching point, although it does contain an evo-  
19 lutionary-branching line along  $X = 0.5$ . Moreover, as indicated by the color coding, this evo-  
20 lutionary-branching line and area induce evolutionary-branching in the direction of niche po-  
21 sition. It is therefore clear that the two identified evolutionary-branching areas are qualitative-  
22 ly different from each other.

## 23 **Comparison with actual evolutionary dynamics**

24 Figure 3b shows occurrences of evolutionary branching in numerically calculated evolution-  
25 ary dynamics, as in Fig. 2b. There exist three clusters: a blue one around the center, a small  
26 red one around  $\mathbf{S} = (0.5, 0.16)^T$ , and a large red one along the bottom of the shown trait  
27 space. Except for the small red cluster, the shapes of these clusters coincide well with the two

1 identified evolutionary-branching areas. Also, as shown by the color coding, the directions of  
2 observed diversifications are predicted well by those areas.

3 As for the blue evolutionary-branching area, the observed process of evolutionary branch-  
4 ing in niche width (dark-yellow curves in Fig. 3b) is always slow, as shown in Fig. 3c. In con-  
5 trast, the large red evolutionary-branching area induces fast and repeated evolutionary branch-  
6 ing in niche position (green curves in Fig. 3b), generating four lineages at the end of the time  
7 window in Fig. 3d. The timescale difference between these two types of branching dynamics  
8 exceeds a factor of 100.

9 This difference in evolutionary speed can be explained as follows. When a population  
10 comes close to the blue evolutionary-branching area, the shape of its niche is similar to the  
11 resource distribution, resulting in weak selection pressures, including disruptive selection. In  
12 this case, the process of evolutionary branching is therefore expected to be slow. On the other  
13 hand, when a population is close to, or located inside, the red evolutionary-branching area, its  
14 niche is much narrower than the resource distribution. This situation creates strong disruptive  
15 selection in niche position. In this case, the process of evolutionary branching is thus expected  
16 to proceed rapidly.

17 This second example shows that our conditions for evolutionary-branching areas can iden-  
18 tify such areas containing no evolutionary-branching point. Here, such an area induces a qual-  
19 itatively different mode of evolutionary branching than the also existing evolutionary-  
20 branching area that contains an evolutionary-branching point. Notice, however, that our con-  
21 ditions for evolutionary-branching areas do not explain the separation between the small and  
22 large red clusters in Fig. 3b. In addition, the size of the blue cluster in Fig. 3b is much larger  
23 than that of the corresponding 20%-threshold area in Fig. 3a, which is not explained either.

### 24 **THIRD EXAMPLE: PREDATOR-PREY MODEL WITH EVOLVING NICHE** 25 **POSITIONS**

26 In this section, based on a predator-prey model, we show that evolutionary branching can oc-  
27 cur even if a model's entire trait space contains no evolutionary-branching point, so that any  
28 occurrence of evolutionary branching is explained by evolutionary-branching lines and areas.

## 1 **Model description**

2 The third model is a modification of the second model towards predator-prey interactions.  
3 This model was developed by Ito *et al.* (2009); see Appendix F for details. As in the first and  
4 second models, trait  $X$  still determines a phenotype's niche position. Now, however, trait  
5  $Y$  is not a niche width as in the second model, but describes the niche position at which the  
6 corresponding phenotype can be consumed as a resource, and is therefore potentially preyed  
7 upon by other phenotypes. We thus refer to  $X$  and  $Y$  as predator-niche position and prey-  
8 niche position, respectively. Accordingly, phenotype  $\mathbf{S}_i$  exists not only as a consumer (pred-  
9 ator) with niche

$$10 \quad c(z, \mathbf{S}_i) = N(z, X_i, \sigma_c^2), \quad (8a)$$

11 but also provides a resource (prey) distribution for predators, with each of its biomass units  
12 contributing according to

$$13 \quad r(z, \mathbf{S}_i) = N(z, Y_i, \sigma_r^2), \quad (8b)$$

14 where the widths of these two distributions are constant and given by  $\sigma_c$  and  $\sigma_r$ , respec-  
15 tively. The basal-resource distribution  $B(z) = R_0 N(z, m_R, \sigma_R^2)$ , with integral  $R_0$ , mean  $m_R$ ,  
16 and standard deviation  $\sigma_R$ , is analogous to the resource distribution in Eq. (7a) for the se-  
17 cond model. In analogy with the second model, the rates of resource gain and biomass loss of  
18 phenotype  $\mathbf{S}_i$ , denoted by  $g(\mathbf{S}_i)$  and  $l(\mathbf{S}_i)$ , respectively, are obtained as overlap integrals  
19 of niches and existing resources. Consequently, the growth rate of phenotype  $\mathbf{S}_i$  is given by

$$20 \quad \frac{dn_i}{dt} = n_i[\lambda g(\mathbf{S}_i) - l(\mathbf{S}_i) - d], \quad (8c)$$

21 where the rate  $d$  of biomass loss by metabolism and natural death is now assumed to be  
22 constant, differently from the second model.

23 As in the second model, we use a simple bivariate normal mutation distribution in which  
24 the standard deviation of mutational step sizes has its maximum  $\sigma_X$  in the  $X$ -direction and  
25 its minimum  $\sigma_Y$  in the  $Y$ -direction.

## 1 Predicted evolutionary-branching lines and areas

2 Figure 4a shows the directional evolution (gray arrows) and predicted evolutionary-branching  
3 lines and areas, as in Fig. 2a and Fig. 3a. This shows that monomorphic populations direc-  
4 tionally evolve so that their prey-niche positions become more distant from their predator-  
5 niche positions, while their predator-niche positions become closer to their prey-niche posi-  
6 tion and/or the mean of the basal-resource distribution (Ito *et al.*, 2009).

7 A unique evolutionarily singular point at  $\mathbf{S} = (0.5, 0.5)^T$  matches the center of the basal-  
8 resource distribution at  $z = m_R = 0.5$ . This corresponds to a cannibalistic population exploit-  
9 ing both the basal resource and itself. As the basal-resource distribution is assumed to be wid-  
10 er than the predator niche,  $\sigma_R > \sigma_c$ , disruptive selection along  $X$  is expected, similarly to  
11 the first example. However, the zero-isocline of the fitness gradient in the  $Y$ -direction (thick  
12 grey curve in Fig. 4a) repels monomorphic populations in the  $Y$ -direction, although the cor-  
13 responding zero-isocline in the  $X$ -direction (thin black curve) attracts them in the  $X$ -  
14 direction. Therefore, depending on the relative mutation probabilities and mutational step siz-  
15 es in  $X$  and  $Y$ , the evolutionarily singular point at the intersection of those two zero-  
16 isoclines may not be convergence stable (Dieckmann and Law, 1996; Leimar, 2009; for anal-  
17 ogous results for multilocus genetics, see Mattessi and Di Pasquale, 1996), in which case  
18 there is no evolutionary-branching point in this trait space.

19 According to our conditions for evolutionary-branching lines, evolutionary branching by  
20 disruptive selection in  $X$  may occur when a phenotype's prey-niche position becomes suffi-  
21 ciently distant from its predator-niche position, so that directional selection on the prey-niche  
22 position becomes sufficiently weak. As thus expected, there exist evolutionary-branching  
23 lines along the evolutionary zero-isocline for  $X$  (red line segments). Evolutionary-  
24 branching areas also exist, but are very thin; only the 20%-threshold areas are sufficiently  
25 large to become visible in Fig. 4a (light-red areas). As shown by the color coding for evolu-  
26 tionary-branching lines and areas, evolutionary branching is solely expected in the direction  
27 of predator-niche position.

1        There also exists a very small evolutionary-branching area around the evolutionarily sin-  
2        gular point at the center, which, however, may induce evolutionary branching only when the  
3        initial phenotype is located within this area, as this singular point is lacking convergence sta-  
4        bility.

## 5        **Comparison with actual evolutionary dynamics**

6        Figure 4b shows occurrences of evolutionary branching in numerically calculated evolution-  
7        ary dynamics, as in Fig. 2b and Fig. 3b. The shapes of the clusters, as well as the directions of  
8        observed evolutionary branching, are predicted well by the evolutionary-branching lines and  
9        areas. Also the sizes of these clusters are predicted well by the 20%-threshold areas.

10        As shown in Fig. 4b (green curves) and Fig. 4d, a monomorphic population first converg-  
11        es to the evolutionary zero-isocline for  $X$  (thin black curve), and then brings about evolu-  
12        tionary branching when it has come sufficiently close to one of the evolutionary-branching  
13        lines.

14        Also, as predicted, evolutionary branching in the small evolutionary-branching area at the  
15        center is possible, provided the initial phenotype is located within this area (dark-yellow  
16        curves in Fig. 4b and Fig. 4c). However, since this evolutionary-branching area is very small  
17        and does not contain an evolutionary attractor, almost all observed diversifications are in-  
18        duced by the identified evolutionary-branching lines.

19        Even when the predator niche is wider than the prey niche and the basal-resource distribu-  
20        tion (  $\sigma_c > \sigma_r, \sigma_R$  ; e.g., when  $\sigma_c = 0.081$  slightly exceeds  $\sigma_r = \sigma_R = 0.08$  , while  
21         $\sigma_x = 0.003$  and  $\sigma_X = 0.0003$  ), evolutionary-branching lines can exist and induce diversifi-  
22        cation (not shown). In any case, the initial evolutionary branching always occurs adjacent to  
23        the evolutionary-branching lines.

24        Interestingly, evolutionary branching in this model can be recurrent: this may result in  
25        complex food webs of coexisting phenotypes, including the evolutionarily stable emergence  
26        of multiple trophic levels (Ito *et al.*, 2009).

## 1 **DISCUSSION**

2 In this study we have presented conditions for evolutionary-branching lines and areas, and  
3 have explored their utility by numerically analyzing evolutionary branching in three different  
4 eco-evolutionary models defined with bivariate trait spaces. The first model, a resource-  
5 competition model with evolving niche positions, has shown how an evolutionary-branching  
6 point transforms into an evolutionary-branching line and elongated evolutionary-branching  
7 area, due to differences in mutational step sizes among the two trait directions. The second  
8 model, a resource-competition model with evolving niche position and niche width, has  
9 shown the existence of an evolutionary-branching line and area containing no evolutionary-  
10 branching point, which induce a qualitatively different mode of evolutionary branching than  
11 the also existing evolutionary-branching point. The third model, a predator-prey model with  
12 evolving predator- and prey-niche positions, has shown that even when a model's entire trait  
13 space contains no evolutionary-branching point, evolutionary branching may still be bound to  
14 occur along evolutionary-branching lines and within evolutionary-branching areas. Below we  
15 discuss these phenomena in greater detail.

16 To understand the transformation of an evolutionary-branching point into an evolutionary-  
17 branching line and an elongated evolutionary-branching area in the first model, it is helpful to  
18 recognize that an evolutionary-branching line becomes straight and infinitely long in the limit  
19 of mutational step sizes parallel to that line converging to 0. In this limit, the resultant evolu-  
20 tionary dynamics are effectively univariate and occur vertically to the evolutionary-branching  
21 line. In the resultant effectively univariate trait space, the evolutionary-branching line then  
22 corresponds to an evolutionary-branching point. Thus, the curvatures and finite lengths of  
23 evolutionary-branching lines can be appreciated as resulting from eco-evolutionary settings  
24 that are intermediate between the two extremes of effectively univariate trait spaces (Metz *et*  
25 *al.*, 1992; Geritz *et al.*, 1997) and fully bivariate ones (Ackermann and Doebeli, 2004; Egas *et*  
26 *al.*, 2005; Vukics and Meszéna, 2003; Ito and Dieckmann, 2007).

27 In our examples, such settings are created by considering different mutational step sizes in  
28 two directions of trait space. Importantly, the very same effects also arise when invasion-

1 fitness functions possess different sensitivities to trait changes in two directions of trait space.  
2 This is simply because such sensitivity differences can be translated into differences in muta-  
3 tional step sizes by suitably rescaling trait space. In many settings, these two types of differ-  
4 ences are formally indistinguishable, and are jointly captured by the local normalization of  
5 trait space we have described. The situation is different when the traits contributing to a mul-  
6 tivariate phenotype happen to be defined on the same, or naturally comparable, scales. In such  
7 special settings, it is feasible to assess whether the emergence of evolutionary-branching lines  
8 and areas is due to differences in mutational steps, differences in fitness sensitivities, or a  
9 combination thereof.

10 The existence of evolutionary-branching lines and areas containing no evolutionary-  
11 branching points, observed in our second and third examples, will go unnoticed by any analy-  
12 sis restricted to identifying evolutionary-branching points. Extending past and future theoreti-  
13 cal studies by accounting for our conditions for evolutionary-branching lines and areas is  
14 therefore advisable, as modes of evolutionary diversification in the underlying models may  
15 otherwise be missed.

16 For instance, our conditions have revealed that if disruptive selection is particularly  
17 strong, evolutionary branching can occur even in the face of considerable directional selec-  
18 tion. This mode is characterized by a rapid progression of the diversification, as illustrated by  
19 our second example when a population's niche is much narrower than the resource distribu-  
20 tion. In this situation, evolutionary branching in niche position is rapidly repeated, accompa-  
21 nied by gradual evolutionary generalization. Consequently, such evolutionary dynamics are  
22 expected to occur also in models examined in previous studies of the joint evolution of niche  
23 position and niche width (Ackerman and Doebeli, 2003; Egas and Dieckmann, 2004; Ito and  
24 Shimada, 2007). Accordingly, this finding could open up new perspectives for understanding  
25 empirically observed instances of adaptive radiation, such as in Darwin's finches (Grant and  
26 Grant, 2008), cichlid fish (Seehausen, 2006), sticklebacks (Bell and Foster, 1994; Schluter,  
27 2000), and anolis lizards (Losos, 2009).

28 Our third model, a predator-prey model with evolving niche positions, illustrates how it is  
29 straightforward to draw qualitative conclusions from our conditions for evolutionary-

1 branching lines and areas. Specifically, when the width of the predator niche is similar to that  
2 of the basal-resource distribution, there can be no particularly strong disruptive selection.  
3 Therefore, directional selection vertical to the disruptive selection needs to be sufficiently  
4 weak if evolutionary branching is to occur. This is possible only when a phenotype's prey-  
5 niche position is distant from its predator-niche position, giving rise to the evolutionary-  
6 branching lines and areas shown in Fig. 4a. Applying our conditions, analogous evolutionary-  
7 branching lines and areas can be identified also in other predator-prey models (Ito and  
8 Ikegami, 2006; Ito *et al.*, 2009) that are comparable to our third model (not shown).

9 In a similar vein, we can consider predator-prey models that differ from our third model.  
10 For example, in the predator-prey model by Brännström *et al.* (2010), the predator-niche and  
11 prey-niche positions are given by a single trait, resulting in a univariate trait space that has a  
12 single evolutionary-branching point. While univariate trait spaces naturally cannot contain  
13 evolutionary-branching lines or areas, our findings here suggest that it will be interesting to  
14 extend the model by Brännström *et al.* (2010) so that the predator-niche and prey-niche posi-  
15 tions can evolve separately: the previously found evolutionary-branching point is then ex-  
16 pected to transform into evolutionary-branching lines and areas, and additional evolutionary-  
17 branching lines and areas containing no evolutionary-branching point might emerge.

18 It may also be worthwhile to revisit, in light of our conditions, a study by Doebeli and  
19 Dieckmann (2000) that also demonstrated evolutionary branching driven by predator-prey  
20 interactions. Their model considered two univariate traits, one for a predator's predator-niche  
21 position and one for a prey's prey-niche position: thus, the predator can adapt only in terms of  
22 its predator-niche position, while the prey can adapt only in terms of its prey-niche position.  
23 Although this doubly univariate setting formally differs from the bivariate setting we have  
24 analyzed in the present study, applying our conditions might help reveal the existence of evo-  
25 lutionary-branching lines and areas in the model by Doebeli and Dieckmann (2000).

26 Our conditions for evolutionary-branching lines and areas are analytically derived from  
27 assessing the potential for immediate evolutionary branching of a monomorphic population  
28 (Ito and Dieckmann, submitted). Since these conditions are sufficient, but not necessary, evo-  
29 lutionary branching in numerically calculated evolutionary dynamics may occur under a wid-

1 er range of conditions, reflecting the gradual integration of local probabilistic rates of evolu-  
2 tionary branching along monomorphic evolutionary trajectories. Accordingly, no full agree-  
3 ment between these two perspectives can be expected. It is therefore encouraging that the re-  
4 sults presented here have demonstrated that the positions and shapes of clusters of occurrenc-  
5 es of evolutionary branching are well predicted by evolutionary-branching areas. Moreover,  
6 the sizes of those clusters are well predicted by the corresponding 20%-threshold areas in  
7 many, but not all, cases (see, e.g., the small blue evolutionary-branching area in Fig. 3a). A  
8 further potential cause of disparity is that our conditions for evolutionary-branching areas use  
9 only partial information about the local selection pressures, assuming that the second-order  
10 derivatives  $C_{yy}$ ,  $C_{xy}$ ,  $C_{yx}$ , and  $D_{yy}$  (as measured in the locally normalized coordinate sys-  
11 tems) are not important. Occasionally, these additional characteristics of the local shapes of  
12 fitness landscapes might well affect the local probabilistic rates of evolutionary branching. A  
13 formal analysis of these effects, if it turned out to be technically feasible, might improve pre-  
14 dictive performance.

15 Our results in this study are based on restrictive assumptions, such as small mutation rates,  
16 large population sizes, bivariate normal mutation distributions, and asexual reproduction. It  
17 will therefore be desirable to examine the robustness of our results by relaxing or varying  
18 those assumptions. First, when mutation rate is large, evolutionary dynamics are no longer  
19 described by trait-substitution sequences, but instead amount to gradual changes of polymor-  
20 phic trait distributions. In this case, one could attempt to define an effective mutation proba-  
21 bility distribution by considering the convolution of the phenotype distribution with the actual  
22 mutation probability distribution. As this convolution is always wider than the actual mutation  
23 probability distribution alone, and as the conditions for evolutionary-branching lines and areas  
24 predict higher likelihoods of evolutionary branching for larger mutational step sizes, large  
25 mutation rates may effectively increase those likelihoods. Second, when population sizes are  
26 not sufficiently large, demographic stochasticity may destroy protected dimorphisms shortly  
27 after their emergence, as the two coexisting phenotypes initially are almost ecologically neu-  
28 tral (Claessen *et al.*, 2007, 2008). This can suppress evolutionary branching. Third, variations  
29 of the mutation probability distribution, keeping its variance-covariance matrix constant, may

1 enhance or suppress the likelihood of evolutionary branching, depending on the specific  
2 shapes considered. Fourth, sexual reproduction is expected to suppress evolutionary branch-  
3 ing, as the continuous production of intermediate offspring phenotypes counteracts diversifi-  
4 cation by disruptive selection (Dieckmann and Doebeli, 1999; Kisdi *et al.*, 1999).

5 As for mutation rates and mutation probability distributions, Ito and Dieckmann (submit-  
6 ted) have already shown that (for  $C_{yy}, C_{xy}, C_{yx}, D_{yy} = 0$  in the normalized coordinate sys-  
7 tems) the derived conditions for evolutionary-branching lines are reasonably robust to making  
8 mutation rates larger and letting mutation distributions deviate from being normal. This ro-  
9 bustness may nevertheless be affected by making population sizes smaller than those already  
10 analyzed, so that demographic stochasticity becomes relatively more important. As for sexual  
11 reproduction, evolutionary branching of sexual populations induced by evolutionary-  
12 branching lines has been demonstrated numerically by Dieckmann and Ito (2007). This pre-  
13 ceding work considered the joint evolution of several quantitative traits, an ecological trait  
14 and mating traits, with additive multilocus genetics, free recombination, and not-small muta-  
15 tion rates. This analysis has demonstrated that when the evolution of assortative mating is  
16 difficult, evolutionary branching will often be suppressed, which implies that sexual repro-  
17 duction may cause likelihoods of evolutionary branching to be overestimated by the condi-  
18 tions reported here for evolutionary-branching lines and areas in asexual populations.

19 Although we have focused on bivariate trait spaces in this study (to facilitate visual in-  
20 spection), the conditions for evolutionary-branching lines derived by Ito and Dieckmann  
21 (submitted) readily apply to multivariate trait spaces, and our conditions for evolutionary-  
22 branching areas generalize analogously. Moreover, our conditions for evolutionary-branching  
23 lines and areas are expected to be applicable also to coevolutionary dynamics and to the dy-  
24 namics of subsequent evolutionary branching after a primary evolutionary branching has oc-  
25 curred. From a computational perspective, it is promising to interleave the application of our  
26 conditions with the time integration of the canonical equation of adaptive dynamics theory  
27 (Dieckmann and Law, 1996): in this way, the deterministic approximation of evolutionary  
28 branching provided by our conditions can be integrated with the deterministic approximation

1 of directional evolutionary and coevolutionary dynamics provided by the canonical equation,  
2 resulting in a deterministic oligomorphic model of phenotypic evolution.

3 In conclusion, our conditions for evolutionary-branching lines and areas have yielded two  
4 new insights into evolutionary branching. First, evolutionary-branching points can transform  
5 into evolutionary-branching lines and areas, due to differences in mutational steps and/or fit-  
6 ness sensitivities among directions in trait spaces. Second, evolutionary-branching lines and  
7 areas can exist independently of evolutionary-branching points, which allows diversification  
8 even when an entire trait space contains not a single evolutionary-branching point.

## 9 **ACKNOWLEDGEMENTS**

10 The authors thank the organizers, participants, and sponsors of the workshop on Niche Theory  
11 and Speciation, which took place in Keszthely, Hungary, in August 2011, and provided the  
12 platform for developing the special issue for which this article has been prepared. The work-  
13 shop was organized under the auspices of the European Research Networking Programme on  
14 Frontiers of Speciation Research (FroSpects), funded by the European Science Foundation.  
15 U.D. gratefully acknowledges financial support by the European Science Foundation, the  
16 Austrian Science Fund, the Austrian Ministry of Science and Research, and the Vienna Sci-  
17 ence and Technology Fund, as well as by the European Commission, through the Marie Curie  
18 Research Training Network FishACE and the Specific Targeted Research Project FinE.

## 19 **REFERENCES**

- 20 Ackermann, M. and Doebeli, M. 2004. Evolution of niche width and adaptive diversification.  
21 *Evolution*, **58**: 2599-2612.
- 22 Beddington, J.R. 1975. Mutual interference between parasites or predators and its effect on  
23 searching efficiency. *J. Anim. Ecol.*, **44**: 331-340.
- 24 Bell, M.A. and Foster, S.A. 1994. *The Evolutionary Biology of the Threespine Stickleback*.  
25 Oxford University Press, Oxford.
- 26 Brännström, Å., Loeuille, N., Loreau, M. and Dieckmann, U. 2011. Emergence and mainte-  
27 nance of biodiversity in an evolutionary food-web model. *Theor. Ecol.*, **4**: 467-478.

- 1 Claessen, D., Andersson, J., Persson, L., and de Roos, A.M. 2007. Delayed evolutionary  
2 branching in small populations. *Evol. Ecol. Res.*, **9**: 51-69.
- 3 Claessen, D., Andersson, J. and Persson, L. 2008. The effect of population size and recombina-  
4 tion on delayed evolution of polymorphism and speciation in sexual populations. *Am.*  
5 *Nat.*, **172**: E18-E34.
- 6 DeAngelis, D.L., Goldstein, R.A. and O'Neill, R.V. 1975. A model for trophic interaction.  
7 *Ecology*, **56**: 881-892.
- 8 Dieckmann, U., Brännström, Å., HilleRisLambers, R. and Ito, H.C. 2007. The adaptive dy-  
9 namics of community structure. In: *Mathematics for Ecology and Environmental Scienc-*  
10 *es*, eds. Takeuchi Y, Sato K and Iwasa Y, pp. 145-177. Springer Verlag, Berlin.
- 11 Dieckmann, U. and Doebeli, M. 1999. On the origin of species by sympatric speciation. *Nat-*  
12 *ure*, **400**: 354-357.
- 13 Dieckmann, U., Doebeli, M., Metz, J.A.J. and Tautz, D. eds. 2004. Adaptive Speciation.  
14 Cambridge University Press, Cambridge.
- 15 Dieckmann, U., Marrow, P. and Law, R. 1995. Evolutionary cycling in predator-prey interac-  
16 tions: population dynamics and the Red Queen. *J. Theor. Biol.*, **176**: 91-102.
- 17 Dieckmann, U. and Law, R. 1996. The dynamical theory of coevolution: a derivation from  
18 stochastic ecological processes. *J. Math. Biol.*, **34**: 579-612.
- 19 Dieckmann, U., Metz, J.A.J., Doebeli, M. and Tautz, D. 2004. Adaptive Speciation. Cam-  
20 bridge University Press, Cambridge.
- 21 Doebeli, M. 1996. A quantitative genetic model for sympatric speciation. *J. Evol. Biol.*, **9**:  
22 893-909.
- 23 Doebeli, M. and Dieckmann, U. 2000. Evolutionary branching and sympatric speciation  
24 caused by different types of ecological interactions. *Am. Nat.*, **156**: S77-S101.
- 25 Doebeli, M. and Dieckmann, U. 2003. Speciation along environmental gradients. *Nature*, **421**:  
26 259-264.
- 27 Durinx, M. and Van Dooren, T.J. 2009. Assortative mate choice and dominance modification:  
28 alternative ways of removing heterozygote disadvantage. *Evolution*, **63**: 334-352.

- 1 Egas, M., Sabelis, M.W. and Dieckmann, U. 2005. Evolution of specialization and ecological  
2 character displacement of herbivores along a gradient of plant quality. *Evolution*, **59**: 507-  
3 520.
- 4 Geritz, S.A.H., Gyllenberg, M., Jacobs, F.J.A. and Parvinen, K. 2002. Invasion dynamics and  
5 attractor inheritance. *J. Math. Biol.*, **44**: 548-560.
- 6 Geritz, S.A.H., Metz, J.A.J., Kisdi, É. and Meszéna, G. 1997. Dynamics of adaptation and  
7 evolutionary branching. *Phys. Rev. Lett.*, **78**: 2024-2027.
- 8 Geritz, S.A.H., Kisdi, É., Meszéna, G. and Metz, J.A.J. 1998. Evolutionarily singular strate-  
9 gies and the adaptive growth and branching of the evolutionary tree. *Evol. Ecol.*, **12**: 35-  
10 57.
- 11 Grant, B.R. and Grant, P. 2008. How and Why Species Multiply: The Radiation of Darwin's  
12 Finches (Princeton Series in Evolutionary Biology), Princeton University Press
- 13 Heinz, S.K., Mazzucco, R. and Dieckmann, U. 2009. Speciation and the evolution of dispersal  
14 along environmental gradients. *Evol. Ecol.*, **23**: 53-70.
- 15 Hendry, A.P. and Kinnison, M.T. 1999. The pace of modern life: measuring rates of contem-  
16 porary microevolution. *Evolution*, **53**: 1637-1653.
- 17 Ito, H.C. and Dieckmann, U. 2007. A new mechanism for recurrent adaptive radiations. *Am.*  
18 *Nat.*, **170**: E96-E111.
- 19 Ito, H.C. and Dieckmann, U. (submitted). Evolutionary branching under slow directional evo-  
20 lution.
- 21 Ito, H.C. and Ikegami, T. 2006. Food web formation through recursive evolutionary branch-  
22 ing. *J. Theor. Biol.*, **238**: 1-10.
- 23 Ito, H.C. and Shimada, M. 2007. Niche expansion: coupled evolutionary branching of niche  
24 position and width. *Evol. Ecol. Res.*, **9**: 675-695.
- 25 Ito, H.C., Shimada, M. and Ikegami, T. 2009. Coevolutionary dynamics of adaptive radiation  
26 for food-web development. *Popul. Ecol.*, **51**: 65-81.
- 27 Kisdi, É. and Geritz, S.A.H. 1999. Adaptive dynamics in allele space: evolution of genetic  
28 polymorphism by small mutations in a heterogeneous environment. *Evolution*, **53**: 993-  
29 1008.

- 1 Kinnison, M.T. and Hendry, A.P. 2001. The pace of modern life II: from rates of contempo-  
2 rary microevolution to pattern and process. *Genetica*, **112-113**: 145-164.
- 3 Leimar, O. 2005. The evolution of phenotypic polymorphism: randomized strategies versus  
4 evolutionary branching. *Am. Nat.*, **165**: 669-681.
- 5 Leimar, O. 2009. Multidimensional convergence stability. *Evol. Ecol. Res.*, **11**: 191-208.
- 6 Losos, J.B. 2009. Lizards in an Evolutionary Tree: Ecology and Adaptive Radiation of  
7 Anoles. University of California Press, Berkeley, CA.
- 8 MacArthur, R. 1972. Geographical Ecology. Harper and Row, New York.
- 9 MacArthur, R. and Levins, R. 1967. The limiting similarity, convergence, and divergence of  
10 coexisting species. *Am. Nat.*, **101**: 377-385.
- 11 Matessi, C. and Di Pasquale, C., 1996. Long term evolution of multi-locus traits. *J. Math.*  
12 *Biol.*, **34**: 613-653.
- 13 Metz, J.A.J., Geritz, S.A.H., Meszéna, G., Jacobs, F.J.A. and van Heerwaarden, J.S. 1996.  
14 Adaptive dynamics: a geometrical study of the consequences of nearly faithful reproduc-  
15 tion. In: van Strien, S.J. and Verduyn-Lunel, S.M. (eds) Stochastic and Spatial Structures  
16 of Dynamical Systems. North Holland, Amsterdam, The Netherlands, pp 183-231.
- 17 Metz, J.A.J., Nisbet, R.M. and Geritz, S.A.H. 1992. How should we define 'fitness' for gen-  
18 eral ecological scenarios? *Trends Ecol. Evol.*, **7**: 198-202.
- 19 Payne, J.L., Mazzucco and R., Dieckmann, U. 2011. The evolution of conditional dispersal  
20 and reproductive isolation along environmental gradients. *J. Theor. Biol.*, **273**: 147-155.
- 21 Ravnigné, V., Dieckmann, U. and Olivieri, I. 2009. Live where you thrive: joint evolution of  
22 habitat choice and local adaptation facilitates specialization and promotes diversity. *Am.*  
23 *Nat.*, **174**: E141-E169.
- 24 Roughgarden, J. 1972. Evolution of niche width. *Am. Nat.*, **106**: 683-718.
- 25 Roughgarden, J. 1974. Species packing and the competition function with illustrations from  
26 coral reef fish. *Theor. Popul. Biol.*, **5**: 163-186.
- 27 Roughgarden, J. 1976. Resource partitioning among competing species: a coevolutionary ap-  
28 proach. *Theor. Popul. Biol.*, **9**: 388-424.
- 29 Schluter, D. 2000. The Ecology of Adaptive Radiation. Oxford University Press, Oxford.

- 1 Seehausen, O. 2006. African cichlid fish: a model system in adaptive radiation research. *Proc.*  
2 *R. Soc. Lond. B*, **273**:1987-1998.
- 3 Vukics, A., Asboth, J. and Meszéna, G. 2003. Speciation in multivariate evolutionary space.  
4 *Phys. Rev. E.*, **68**: 041903.

## 5 **FIGURE CAPTIONS**

6 **Figure 1.** Illustration of the local characteristics of an evolutionary-branching line. For check-  
7 ing the conditions for an evolutionary-branching line (grey line), the trait space  $(X,Y)$   
8 (frame axes) is locally normalized so that in the new coordinates  $(x,y)$  (black lines) muta-  
9 tional steps are isotropic and disruptive selection is maximal in the direction of  $x$ . If at a  
10 phenotype  $S_0$  the maximum disruptive selection  $D_{xx}$  in the direction of  $x$  is sufficiently  
11 strong compared to the directional selection  $G_y$  in the direction of  $y$ , and if  $S_0$  is moreover  
12 convergence stable in the direction of  $x$ , then an evolutionary branching-line is passing  
13 through  $S_0$ .

14 **Figure 2.** Prediction and observation of evolutionary-branching lines and areas in a resource-  
15 competition model with evolving bivariate niche positions and non-isotropic mutational steps.  
16 (a) Predicted evolutionary-branching line, evolutionary-branching area, and 20%-threshold  
17 area, depicted by a line segment and by two nested areas filled with dark and light colors, re-  
18 spectively. The colors of the line and areas follow a red-blue gradation indicating the predict-  
19 ed directions of evolutionary branching: pure red and pure blue correspond to evolutionary  
20 branching in the directions of the  $X$ -axis and  $Y$ -axis, respectively. Gray arrows indicate the  
21 directional evolution of monomorphic populations. The black and gray lines are zero-isoclines  
22 of the fitness gradient in the directions of the traits  $X$  and  $Y$ , respectively. (b) Occurrences  
23 of evolutionary branching (triangles) in numerically calculated evolutionary dynamics starting  
24 from 200 phenotypes randomly chosen from a uniform distribution across the shown trait  
25 space. Observed directions of evolutionary branching are indicated by the same colors as in  
26 (a). To facilitate comparison, the dashed curve repeats the boundary of the 20%-threshold area  
27 from (a). Two example trajectories of evolutionary dynamics are shown as dark-yellow and

1 green curves, respectively, with initial phenotypes marked by the letters ‘c’ and ‘d.’ These  
 2 marks match the panels on the right, showing evolutionary dynamics over time, with thick  
 3 and thin curves corresponding to the traits  $X$  and  $Y$ , respectively. Filled circles in (b) indi-  
 4 cate the final phenotypes shown in (c) and (d), while filled triangles in (b) indicate the pheno-  
 5 types at which evolutionary branching occurs in the two example trajectories. Parameters:  
 6  $\sigma_K = 0.8$ ,  $\sigma_a = 0.5$ ,  $K_0 = 1000$ ,  $\varepsilon_e = 10^{-5}$ ,  $\mu = 10^{-5}$ ,  $\sigma_1 = 0.01$ ,  $\sigma_2 = 0.003$ .

7 **Figure 3.** Prediction and observation of evolutionary-branching lines and areas in a resource-  
 8 competition model with evolving niche positions and widths. (a) Predicted evolutionary-  
 9 branching line (red line at the center bottom), evolutionary-branching areas (red and small  
 10 blue areas), and 20%-threshold areas (light-red and light-blue areas). Other elements are as in  
 11 Fig. 2a. The inset shows a magnified view of the evolutionary-branching areas and corre-  
 12 sponding 20%-threshold area around the evolutionary-branching point at  $(X, Y) = (0, 0.282)$ .  
 13 (b) Occurrences of evolutionary branching (triangles) in numerically calculated evolutionary  
 14 dynamics starting from 700 phenotypes randomly chosen from a uniform distribution across  
 15 the shown trait space. Two example trajectories of evolutionary dynamics are shown as in  
 16 Figs. 2b. Other elements are as in Fig. 2b. Parameters:  $\sigma_R = 0.2$ ,  $m_R = 60$ ,  $R_0 = 400$ ,  
 17  $\lambda = 0.3$ ,  $\alpha = \beta = \gamma = 1$ ,  $d_0 = 0.1$ ,  $d_1 = 0.5$ ,  $\varepsilon_e = 10^{-5}$ ,  $\mu = 10^{-5}$ ,  $\sigma_X = 0.01$ ,  $\sigma_Y = 0.003$   
 18 ( $\alpha$ ,  $\beta$ , and  $\gamma$  are introduced in Appendix D, while  $d_0$  and  $d_1$  are introduced in Appendix  
 19 E).

20 **Figure 4.** Prediction and observation of evolutionary-branching lines and areas in a predator-  
 21 prey model with evolving predator-niche and prey-niche positions. (a) Predicted evolutionary-  
 22 branching lines (red lines), evolutionary-branching areas (red areas), and 20%-threshold areas  
 23 (light-red areas). Other elements are as in Figs. 2a and 3a. (b) Occurrences of evolutionary  
 24 branching (triangles) in numerically calculated evolutionary dynamics starting from 200 phe-  
 25 notypes randomly chosen from a uniform distribution across the shown trait space. Two ex-  
 26 ample trajectories of evolutionary dynamics are shown as in Fig. 2b and 3b. Other elements  
 27 are as in Figs. 2b and 3b. Parameters:  $\sigma_c = \sigma_r = 0.06$ ,  $\sigma_R = 0.08$ ,  $R_0 = 4000$ ,  $m_R = 60$ ,

1  $\lambda = 0.3$ ,  $\alpha = 5$ ,  $\beta = \gamma = 1$ ,  $d = 0.1$ ,  $\varepsilon_e = 10^{-5}$ ,  $\mu = 10^{-5}$ ,  $\sigma_x = 0.003$ ,  $\sigma_y = 0.001$  ( $\alpha$ ,  $\beta$ ,  
2 and  $\gamma$  are introduced in Appendix D).

### 3 **APPENDIX A: MUTATION PROBABILITY DISTRIBUTIONS**

4 Here we explain how the mutation probability distributions used in our three examples are  
5 defined and interpreted in terms of mutational step sizes. For all three examples, we define the  
6 mutation probability distributions as bivariate normal distributions in the original coordinate  
7 system  $\mathbf{S} = (X, Y)^T$ ,

$$8 \quad M(\delta\mathbf{S}) = \exp(-\frac{1}{2} \delta\mathbf{S}^T \mathbf{\Lambda}^{-1} \delta\mathbf{S}) / (2\pi \sqrt{\det \mathbf{\Lambda}}), \quad (\text{A1a})$$

9 where  $\mathbf{\Lambda}$  is the mutational variance-covariance matrix, given by

$$10 \quad \mathbf{\Lambda} = \begin{pmatrix} \sigma_x^2 & \sigma_{xy}^2 \\ \sigma_{xy}^2 & \sigma_y^2 \end{pmatrix} = \iint \begin{pmatrix} X^2 & XY \\ XY & Y^2 \end{pmatrix} M(\mathbf{S}) dXdY. \quad (\text{A1b})$$

11 The two eigenvalues of the symmetric matrix  $\mathbf{\Lambda}$  are real and give the maximum and mini-  
12 mum variances of mutational step sizes, and the two corresponding eigenvectors give the di-  
13 rections in which these extrema are attained.

14 For the first model,  $\mathbf{\Lambda}$  is given by

$$15 \quad \mathbf{\Lambda} = \mathbf{P}_\Lambda \begin{pmatrix} \sigma_1^2 & 0 \\ 0 & \sigma_2^2 \end{pmatrix} \mathbf{P}_\Lambda^{-1}, \quad (\text{A2})$$

$$\mathbf{P}_\Lambda = \frac{1}{\sqrt{2}} \begin{pmatrix} -1 & 1 \\ 1 & 1 \end{pmatrix} = \frac{1}{\sqrt{2}} (\mathbf{e}_1, \mathbf{e}_2),$$

16 with  $\sigma_1 \geq \sigma_2 > 0$ . Accordingly, the standard deviation of mutational step sizes has its maxi-  
17 mum  $\sigma_1$  in the direction of  $\mathbf{e}_1 = (-1, 1)^T$ , and its minimum  $\sigma_2$  in the direction of  
18  $\mathbf{e}_2 = (1, 1)^T$ . For the second and third model,  $\mathbf{\Lambda}$  is given by  $((\sigma_x^2, 0), (0, \sigma_y^2))^T$ , with  
19  $\sigma_x \geq \sigma_y > 0$ .

1 **APPENDIX B: CONDITIONS FOR PROTECTED DIMORPHISMS FOR DIS-**  
2 **RUPTIVE SELECTION PARALLEL TO DIRECTIONAL SELECTION**

3 Here we derive conditions for the emergence of protected dimorphisms along maximum-  
4 likelihood-invasion paths (MLIPs) for settings in which the maximum disruptive selection is  
5 parallel to directional selection in the locally normalized coordinate system. We first examine  
6 which mutants in such settings create maximum-likelihood invasions (MLI mutants), which  
7 then enables us to derive the aforementioned conditions.

8 We consider a locally normalized coordinate system  $\mathbf{s} = (x, y)^T$  with origin at  $\mathbf{S}_0$ , in  
9 which akin to Eqs. (1) the normalized invasion-fitness function is expressed as

$$\begin{aligned}
 f(\mathbf{s}'; \mathbf{s}) &= G_x \delta x + G_y \delta y \\
 &+ \frac{1}{2} C_{xx} x \delta x + \frac{1}{2} C_{yy} y \delta y + \frac{1}{2} C_{xy} x \delta y + \frac{1}{2} C_{yx} y \delta x \\
 &+ \frac{1}{2} D_{xx} \delta x^2 + \frac{1}{2} D_{yy} \delta y^2.
 \end{aligned}
 \tag{B1a}$$

11 As before, we assume that  $\mathbf{s}$  is under disruptive selection and that the strength of disruptive  
12 selection is maximal along the  $x$ -axis ( $D_{xx} > 0$ ).

13 We assume that the resident is located at the origin,  $\mathbf{s} = (0, 0)^T$ , corresponding to  $\mathbf{S}_0$ ,  
14 without loss of generality. Because directional selection is assumed to be parallel to the direc-  
15 tion of maximum disruptive selection, we can infer that  $G_y = 0$ . Then,  $x, y = 0$  and Eq.  
16 (B1a) reduces to

$$f(\mathbf{s}'; \mathbf{s}) = G_x \delta x + \frac{1}{2} D_{xx} \delta x^2 + \frac{1}{2} D_{yy} \delta y^2.
 \tag{B1b}$$

18 According to Dieckmann and Law (1996) and Ito and Dieckmann (submitted), the probability  
19 for mutant  $\mathbf{s}'$  to invade resident  $\mathbf{s}$  is given by

$$P(\mathbf{s}'; \mathbf{s}) = T \mu \hat{n} M(\delta \mathbf{s}) f(\mathbf{s}'; \mathbf{s})_+,
 \tag{B2a}$$

21 where  $T$  is a normalization ensuring  $\int P(\mathbf{s}'; \mathbf{s}) d\mathbf{s}' = 1$ , and the subscript “+” indicates the  
22 conversion of negative values  $h$  to 0. Below, we can omit this subscript since we focus on the  
23 maximum of  $P(\mathbf{s}'; \mathbf{s})$ , for which  $f(\mathbf{s}'; \mathbf{s})$  always is positive. In this normalized trait space,  
24 the distribution  $M(\delta \mathbf{s})$  of mutational steps  $\delta \mathbf{s}$  is given by an isotropic bivariate normal

1 distribution,  $M(\delta\mathbf{s}) = N(\delta x, 0, \sigma^2)N(\delta y, 0, \sigma^2)$ . Substituting this and Eq. (B1b) into Eq.  
 2 (B2a) yields

$$3 \quad P(\mathbf{s}'; \mathbf{s}) = A \exp\left(-\frac{\delta x^2 + \delta y^2}{2\sigma^2}\right) \left[ G_x \delta x + \frac{1}{2} D_{xx} \delta x^2 + \frac{1}{2} D_{yy} \delta y^2 \right], \quad (\text{B2b})$$

4 where  $A = \mu \hat{n} T / (2\pi\sigma^2)$ . The mutant with maximum likelihood of invasion (MLI mutant),  
 5 denoted by  $\mathbf{s}'_{\text{MLI}} = (x'_{\text{MLI}}, y'_{\text{MLI}})^T$ , maximizes  $P(\mathbf{s}'; \mathbf{s})$ . The mutational step taken by the MLI  
 6 mutant is  $\delta\mathbf{s}_{\text{MLI}} = (\delta x_{\text{MLI}}, \delta y_{\text{MLI}})^T = \mathbf{s}'_{\text{MLI}} - \mathbf{s}$ . For convenience, we express mutational steps in  
 7 polar coordinate  $(\delta x, \delta y)^T = (\varepsilon \cos \theta, \varepsilon \sin \theta)^T$ , which yields

$$8 \quad \begin{aligned} P(\mathbf{s}'; \mathbf{s}) &= A \exp\left(-\frac{\varepsilon^2}{2\sigma^2}\right) \left[ G_x \varepsilon \cos \theta + \frac{1}{2} D_{xx} \varepsilon^2 \cos^2 \theta + \frac{1}{2} D_{yy} \varepsilon^2 \sin^2 \theta \right] \\ &= A \exp\left(-\frac{\varepsilon^2}{2\sigma^2}\right) \left[ \frac{1}{2} D_{yy} \varepsilon^2 + \frac{1}{2} (D_{xx} - D_{yy}) \varepsilon^2 \cos^2 \theta + G_{xx} \varepsilon \cos \theta \right]. \end{aligned} \quad (\text{B2c})$$

9 Notice that  $D_{xx} - D_{yy} > 0$ , because disruptive selection is maximal in the direction of  $x$ . As  
 10  $\cos \theta$  is maximal and minimal at  $\theta = 0$  and  $\theta = \pi$ , respectively, while  $\cos^2 \theta$  is maximal  
 11 at  $\theta = 0$  and  $\theta = \pi$ , the invasion probability above has its maximum at  $\theta = 0$  for positive  
 12  $G_{xx} \varepsilon$  and at  $\theta = \pi$  for negative  $G_{xx} \varepsilon$ . Thus, the MLI mutant fulfills  $\delta y_{\text{MLI}} = 0$  and  $\delta x_{\text{MLI}}$   
 13 is given by the  $\delta x$  that maximizes

$$14 \quad \bar{P}(\mathbf{s}'; \mathbf{s}) = A \exp\left(-\frac{\delta x^2}{2\sigma^2}\right) \left[ G_x \delta x + \frac{1}{2} D_{xx} \delta x^2 \right]. \quad (\text{B2d})$$

15 The terms above are symmetric with respect to the sign of  $\delta x$ , except for  $G_x \delta x$ . Therefore,  
 16 when  $G_x$  is positive,  $\bar{P}(\mathbf{s}'; \mathbf{s})$  for any negative  $\delta x$  is smaller than  $\bar{P}(\mathbf{s}'; \mathbf{s})$  for a positive  
 17  $\delta x$  with the same absolute value. Thus,  $\delta x_{\text{MLI}} > 0$  holds for  $G_x > 0$ . Analogously,  
 18  $\delta x_{\text{MLI}} < 0$  holds for  $G_x < 0$ .

19 In addition,  $\delta x = \delta x_{\text{MLI}}$  has to fulfill

$$20 \quad \frac{\partial \bar{P}(\mathbf{s}'; \mathbf{s})}{\partial \delta x} = A \frac{1}{\sigma^2} \exp\left(-\frac{\delta x^2}{2\sigma^2}\right) \left[ G_x (\sigma^2 - \delta x^2) + \frac{1}{2} D_{xx} \delta x (2\sigma^2 - \delta x^2) \right] = 0. \quad (\text{B3})$$

21 For positive  $G_x$ , this requires  $\sigma \leq \delta x_{\text{MLI}} \leq \sqrt{2}\sigma$  (because  $D_{xx} \delta x_{\text{MLI}} > 0$ , as  $D_{xx}$  is as-  
 22 summed to be positive and  $\delta x_{\text{MLI}} > 0$  for  $G_x > 0$ ). For negative  $G_x$ , similarly,

1  $-\sqrt{2}\sigma \leq \delta x_{\text{MLI}} \leq -\sigma$  is required (because then  $D_{\text{xx}} \delta x_{\text{MLI}} < 0$ ). In summary, the MLI mutant  
 2 thus always fulfills  $\sigma \leq |\delta x_{\text{MLI}}| \leq \sqrt{2}\sigma$  and  $\delta y_{\text{MLI}} = 0$ .

3 On the basis of these features of MLI mutants, we now examine whether the MLI mutant  
 4 and the considered resident can coexist. The conditions for protected dimorphism are given by  
 5 conditions for mutual invasibility,  $f(\mathbf{s}'_{\text{MLI}}; \mathbf{s}) > 0$  and  $f(\mathbf{s}; \mathbf{s}'_{\text{MLI}}) > 0$ . By substituting  
 6  $\mathbf{s}'_{\text{MLI}} = (\delta x_{\text{MLI}} + x, y)^T$  and  $x = y = 0$  into Eq. (B1a), these conditions are expressed as

$$7 \quad f(\mathbf{s}'_{\text{MLI}}; \mathbf{s}) = G_x \delta x_{\text{MLI}} + \frac{1}{2} D_{\text{xx}} \delta x_{\text{MLI}}^2 > 0, \quad (\text{B4a})$$

8 and

$$9 \quad f(\mathbf{s}; \mathbf{s}'_{\text{MLI}}) = -G_x \delta x_{\text{MLI}} - \frac{1}{2} C_{\text{xx}} \delta x_{\text{MLI}}^2 + \frac{1}{2} D_{\text{xx}} \delta x_{\text{MLI}}^2 > 0. \quad (\text{B4b})$$

10 If

$$11 \quad C_{\text{xx}} < 0, \quad (\text{B5})$$

12 a sufficient condition for inequalities (B4) to be fulfilled is given by

$$13 \quad \frac{|\delta x_{\text{MLI}}| D_{\text{xx}}}{2|G_x|} > 1. \quad (\text{B6})$$

14 As  $\sigma \leq |\delta x_{\text{MLI}}| \leq \sqrt{2}\sigma$ , a sufficient condition for this inequality to be fulfilled is given by

$$15 \quad \frac{\sigma D_{\text{xx}}}{2|G_x|} > 1. \quad (\text{B7})$$

## 16 **APPENDIX C: IDENTIFYING EVOLUTIONARY-BRANCHING LINES AND** 17 **AREAS**

### 18 **General procedure**

19 Here we explain how to identify evolutionary-branching lines and areas in an arbitrary trait  
 20 space, according to Ito and Dieckmann (submitted). For checking conditions for evolutionary-  
 21 branching lines in an arbitrary trait space  $\mathbf{S}$ , the vector  $\mathbf{G}$  and the matrices  $\mathbf{C}$  and  $\mathbf{D}$  of  
 22 the locally normalized invasion-fitness function  $f(\mathbf{s}'; \mathbf{s})$  are all that is needed. To obtain the-

1 se vector and matrices, the trait space  $\mathbf{S}$  is first transformed so that mutational steps become  
 2 isotropic, and then it is further rotated so that  $\mathbf{D}$  becomes diagonal. Specifically,  $F(\mathbf{S}';\mathbf{S})$   
 3 is approximated as the normalized invasion-fitness function, Eq. (1a),

$$4 \quad F(\mathbf{S}';\mathbf{S}) = \check{\mathbf{G}} \delta\mathbf{S} + \frac{1}{2}(\mathbf{S} - \mathbf{S}_0)^T \check{\mathbf{C}} \delta\mathbf{S} + \frac{1}{2} \delta\mathbf{S}^T \check{\mathbf{D}} \delta\mathbf{S}, \quad (\text{C1a})$$

5 where

$$6 \quad \begin{aligned} \check{\mathbf{G}} &= \mathbf{F}_{\mathbf{S}'}, \\ \check{\mathbf{C}} &= \mathbf{F}_{\mathbf{S}'\mathbf{S}'} - \mathbf{F}_{\mathbf{SS}} + \mathbf{F}_{\mathbf{SS}'} - \mathbf{F}_{\mathbf{SS}'}, \\ \check{\mathbf{D}} &= \mathbf{F}_{\mathbf{S}'\mathbf{S}'}, \end{aligned} \quad (\text{C1b})$$

7 with

$$8 \quad \begin{aligned} \mathbf{F}_{\mathbf{S}'} &= (F_{X'} \quad F_{Y'})_{\mathbf{S}'=\mathbf{S}=\mathbf{S}_0}, \\ \mathbf{F}_{\mathbf{S}'\mathbf{S}'} &= \begin{pmatrix} F_{X'X'} & F_{X'Y'} \\ F_{X'Y'} & F_{Y'Y'} \end{pmatrix}_{\mathbf{S}'=\mathbf{S}=\mathbf{S}_0}, \quad \mathbf{F}_{\mathbf{SS}} = \begin{pmatrix} F_{XX} & F_{XY} \\ F_{XY} & F_{YY} \end{pmatrix}_{\mathbf{S}'=\mathbf{S}=\mathbf{S}_0}, \quad \mathbf{F}_{\mathbf{SS}'} = \begin{pmatrix} F_{XX'} & F_{XY'} \\ F_{YX'} & F_{YY'} \end{pmatrix}_{\mathbf{S}'=\mathbf{S}=\mathbf{S}_0}, \end{aligned} \quad (\text{C1c})$$

9 where  $F_\alpha$  for  $\alpha = X', Y', X, Y$  and  $F_{\alpha\beta}$  for  $\alpha, \beta = X', Y', X, Y$  denote the first and second  
 10 partial derivatives of  $F(\mathbf{S}';\mathbf{S})$  with respect to  $\alpha$  and  $\beta$ , respectively.

11 By locally normalizing the trait space through an affine transformation, i.e., by substitut-  
 12 ing  $\mathbf{S} - \mathbf{S}_0 = \mathbf{Q}^T \mathbf{B} \mathbf{s}$  and  $\delta\mathbf{S} = \mathbf{Q}^T \mathbf{B} \delta\mathbf{s}$  into Eq. (C1a) and comparing with Eq. (1a), we see  
 13 that  $\mathbf{G}$ ,  $\mathbf{C}$  and  $\mathbf{D}$  are given by

$$14 \quad \begin{aligned} \mathbf{G} &= \check{\mathbf{G}} \mathbf{Q}^T \mathbf{B}, \\ \mathbf{C} &= \mathbf{B}^T \mathbf{Q} \check{\mathbf{C}} \mathbf{Q}^T \mathbf{B}, \\ \mathbf{D} &= \mathbf{B}^T \mathbf{Q} \check{\mathbf{D}} \mathbf{Q}^T \mathbf{B}. \end{aligned} \quad (\text{C2a})$$

15 The matrix  $\mathbf{Q}$  describes the scaling of mutational step sizes to make them isotropic,

$$16 \quad \mathbf{Q} = \frac{1}{\sigma} \begin{pmatrix} \sigma_X & \sigma_{XY}^2 / \sigma_X \\ 0 & \sqrt{\sigma_X^2 \sigma_Y^2 - \sigma_{XY}^4} / \sigma_X \end{pmatrix}, \quad (\text{C2b})$$

17 where  $\sigma_X^2$ ,  $\sigma_Y^2$ , and  $\sigma_{XY}^2$  are the components of the mutational variance-covariance matrix  
 18  $\mathbf{\Lambda}$ , and  $\sigma^2$  is the dominant eigenvalue of  $\mathbf{\Lambda}$ , measuring the maximum variance of muta-  
 19 tional step sizes among all directions in trait spaces. The matrix  $\mathbf{Q}$  can be obtained as the

1 Cholesky decomposition of  $\Lambda/\sigma^2$ ,  $\Lambda/\sigma^2 = \mathbf{Q}^T \mathbf{Q}$ , with  $\mathbf{Q}$  having upper-triangular form.  
 2 The matrix  $\mathbf{B}$  describes the rotation of the trait axes to align them with the direction of maximum disruptive selection,

$$3 \quad \mathbf{B} = (\mathbf{v}_1, \mathbf{v}_2), \quad (\text{C2c})$$

5 where  $\mathbf{v}_1$  and  $\mathbf{v}_2$  are the eigenvectors of  $\mathbf{Q}\mathbf{D}\mathbf{Q}^T$ , ordered so that the corresponding eigenvalues fulfill  $\lambda_1 > \lambda_2$ , which makes  $\mathbf{D}$  diagonal with  $D_{xx} > D_{yy}$ .

7 By substituting Eqs. (C2) into the conditions for evolutionary-branching lines, Eqs. (2a-c),  
 8 the set of phenotypes  $\mathbf{S}_0$  fulfilling those conditions is found, thus yielding the evolutionary-  
 9 branching lines.

## 10 Illustrative example

11 Here we elaborate on the illustrative analysis of evolutionary-branching lines and areas  
 12 around an evolutionary-branching point in the simple example briefly explained in the subsection  
 13 “Sizes and shapes of evolutionary-branching lines and areas” in the main text.

14 As explained there, we suppose that a trait space  $\mathbf{S} = (X, Y)^T$  possesses an evolutionary-  
 15 branching point at its origin. For a point  $\mathbf{S}_0$  close to the origin, the invasion-fitness function  
 16  $F(\mathbf{S}'; \mathbf{S})$  can be expanded as shown in Eq. (C1a). By further expanding  $\check{\mathbf{G}}$ ,  $\check{\mathbf{C}}$ , and  $\check{\mathbf{D}}$  in  
 17 terms of  $\mathbf{S}_0$  around the origin, these are approximately given by

$$18 \quad \check{\mathbf{G}} = \check{\check{\mathbf{G}}} + \mathbf{S}_0^T \check{\check{\mathbf{C}}}, \quad \check{\mathbf{C}} = \check{\check{\mathbf{C}}}, \quad \text{and} \quad \check{\mathbf{D}} = \check{\check{\mathbf{D}}}, \quad (\text{C3})$$

19 where  $\check{\check{\mathbf{G}}}$ ,  $\check{\check{\mathbf{C}}}$ , and  $\check{\check{\mathbf{D}}}$  denote the matrices  $\check{\mathbf{G}}$ ,  $\check{\mathbf{C}}$ , and  $\check{\mathbf{D}}$  at  $\mathbf{S}_0 = (0, 0)^T$ , respectively.

20 For the origin to be an evolutionarily singular point,  $\check{\check{\mathbf{G}}} = \mathbf{0}$  is required. For the sake of illustration,  
 21 we assume that  $\check{\check{\mathbf{D}}} = ((D_{xx}, 0), (0, D_{yy}))^T$ ,  $D_{xx} \geq D_{yy}$ , and  $\check{\check{\mathbf{C}}} = ((C_{xx}, 0), (0, C_{yy}))^T$ .

22 And for the origin to be an evolutionary-branching point, we assume that it is strongly convergence stable,  
 23  $C_{xx}, C_{yy} < 0$ , and that it is not evolutionarily stable,  $D_{xx} > 0$ . In addition,  
 24 we assume that mutational steps in the traits  $X$  and  $Y$  have no correlation,  $\sigma_{xy} = 0$ , and  
 25 are largest along the  $X$ -axis,  $\sigma_x \geq \sigma_y$ . Then, the matrices  $\mathbf{Q}$  and  $\mathbf{B}$  are given by the  
 26 constant matrices,

$$1 \quad \mathbf{Q} = \begin{pmatrix} 1 & 0 \\ 0 & \sigma_Y / \sigma_X \end{pmatrix} \quad \text{and} \quad \mathbf{B} = \begin{pmatrix} 1 & 0 \\ 0 & 1 \end{pmatrix}, \quad (C4)$$

2 with  $\sigma = \sigma_X$ . Substituting Eqs. (C3) and (C4) into Eqs. (C2a) yields

$$3 \quad \begin{aligned} \mathbf{G} &= (G_x \quad G_y) = (C_{XX}X_0 \quad rC_{YY}Y_0), \\ \mathbf{C} &= \begin{pmatrix} C_{xx} & C_{xy} \\ C_{yx} & C_{yy} \end{pmatrix} = \begin{pmatrix} C_{XX} & 0 \\ 0 & r^2C_{YY} \end{pmatrix}, \\ \mathbf{D} &= \begin{pmatrix} D_{xx} & D_{xy} \\ D_{xy} & D_{yy} \end{pmatrix} = \begin{pmatrix} D_{XX} & 0 \\ 0 & r^2D_{YY} \end{pmatrix}, \end{aligned} \quad (C5)$$

4 with  $r = \sigma_Y / \sigma_X$ . Substituting Eqs. (C5) into the conditions for evolutionary-branching lines  
5 and areas, Eqs. (2) and (3a), then yields Eqs. (4) and (5).

## 6 **APPENDIX D: FUNCTIONAL RESPONSE IN SECOND AND THIRD MOD-** 7 **ELS**

8 Here we explain how the functional response used in the second and third model is derived.  
9 Extending results by Beddington (1975) and DeAngelis *et al.* (1975), we start by deriving the  
10 functional response of phenotype  $\mathbf{S}$  to resource type  $z$ ,

$$11 \quad g_R(z, \mathbf{S}) = \phi(\mathbf{S})Ac(z, \mathbf{S})e_R R(z), \quad (D1a)$$

12 where  $\phi(\mathbf{S})$  is the search effort per consumption effort,  $A$  is the total rate of consumption  
13 effort, and  $c(z, \mathbf{S})$  describes the probability density of consumption effort over resources  
14 types  $z$  by phenotype  $\mathbf{S}$  per unit of its biomass. Thus,  $\phi(\mathbf{S})Ac(z, \mathbf{S})$  is the probability  
15 density of search effort per unit time invested on resource type  $z$  by phenotype  $\mathbf{S}$  per unit  
16 of its biomass (search effort for short). As a first-order approximation, the encounter rate of  
17 phenotype  $\mathbf{S}$  with resource type  $z$  is assumed to be proportional to this search effort and to  
18 the density  $R(z)$  of resource type  $z$ , resulting in the proportionality constant  $e_R$ .

19 The first-order approximation is also applied to the rate of interference competition experi-  
20 enced by phenotype  $\mathbf{S}$  while consuming resource type  $z$ ,

$$21 \quad g_C(z, \mathbf{S}) = \phi(\mathbf{S})Ac(z, \mathbf{S})e_C C(z), \quad (D1b)$$

1 which is thus assumed to be proportional to the search effort and to the total consumption  
 2 effort  $C(z)$  invested on resource type  $z$  by all phenotypes, with a proportionality constant  
 3  $e_c$ .  $C(z)$  is given by

$$4 \quad C(z) = A \sum_{j=1}^L n_j c(z, \mathbf{S}_j). \quad (\text{D2})$$

5 The sum of energy invested into resource search, resource handling, and interference  
 6 competition, measured in terms of rates and integrated over all resource types  $z$ , equals the  
 7 total rate  $A$  of consumption effort,

$$8 \quad \int \phi(\mathbf{S}) A c(z, \mathbf{S}) dz + \int h_r g_r(z, \mathbf{S}) dz + \int h_c g_c(z, \mathbf{S}) dz = A, \quad (\text{D3})$$

9 where  $h_r$  and  $h_c$  scale the energy requirements for resource handling and interference  
 10 competition relative to those for resource search. Here it is assumed that these relative energy  
 11 requirements do not depend on resource type, and that they are not complicated by spatial  
 12 population structure. Substituting Eqs. (D1) into Eq. (D2) yields

$$13 \quad \phi(\mathbf{S}) = \frac{1}{1 + h_r e_r \tilde{R}(\mathbf{S}) + h_c e_c \tilde{C}(\mathbf{S})}, \quad (\text{D4})$$

14 and substituting this into Eq. (D1a) yields

$$15 \quad g_r(z, \mathbf{S}) = \frac{A c(z, \mathbf{S}) R(z)}{\alpha + \beta \tilde{R}(\mathbf{S}) + \gamma \tilde{C}(\mathbf{S})}, \quad (\text{D5})$$

16 where

$$17 \quad \tilde{R}(\mathbf{S}) = \int c(z, \mathbf{S}) R(z) dz, \quad \tilde{C}(\mathbf{S}) = \int c(z, \mathbf{S}) C(z) dz, \quad (\text{D6})$$

18  $\alpha = 1/e_r$ ,  $\beta = h_r$ , and  $\gamma = h_c e_c / e_r$ . Integrating Eq. (D4) over all resource types  $z$ ,  
 19  $g(\mathbf{S}) = \int g_r(z, \mathbf{S}) dz$ , finally yields the sought functional response,

$$20 \quad g(\mathbf{S}) = \frac{A \tilde{R}(\mathbf{S})}{\alpha + \beta \tilde{R}(\mathbf{S}) + \gamma \tilde{C}(\mathbf{S})}. \quad (\text{D7})$$

21 Here the parameters  $\alpha$ ,  $\beta$ , and  $\gamma$  measure, respectively, the costs for resource search,  
 22 resource handling, and interference competition.

## 1 APPENDIX E: INVASION FITNESS IN SECOND MODEL

2 Here we derive the invasion-fitness function for the second model. First, for the functional  
3 response in Eq. (D7) we need to specify the total amounts of resource and competitors en-  
4 countered by phenotype  $\mathbf{S}_i$ ,  $\tilde{R}(\mathbf{S}_i)$  and  $\tilde{C}(\mathbf{S}_i)$ , which according to Eq. (D6) are given by  
5 the following overlap integrals,

$$6 \quad \begin{aligned} \tilde{R}(\mathbf{S}_i) &= \int c(z, \mathbf{S}_i) R(z) dz = R_0 N(X_i, m_R, Y_i^2 + \sigma_R^2), \\ \tilde{C}(\mathbf{S}_i) &= \int c(z, \mathbf{S}_i) C(z) dz = A \sum_{j=1}^L n_j N(X_i, X_j, Y_i^2 + Y_j^2), \end{aligned} \quad (\text{E1})$$

7 where  $C(z)$  is the total consumption effort invested on resource type  $z$  by all phenotypes  
8  $\mathbf{S}_j$ , as given by Eq. (D2).

9 Second, we describe the costs of specialization or generalization by an additional death  
10 rate that linearly varies with the niche width  $Y$  of a phenotype  $\mathbf{S}$ ,

$$11 \quad d(Y) = d_0 - d_1 Y, \quad (\text{E2})$$

12 as specified by the two parameters  $d_0$  and  $d_1$ : a positive  $d_1$  results in a cost of  
13 specialization, whereas a negative  $d_1$  results in a cost of generalization.

14 Third, for a monomorphic population with phenotype  $\mathbf{S}$  and equilibrium biomass  $\hat{n}$ , the  
15 invasion fitness of a mutant with phenotype  $\mathbf{S}'$  is then derived according to Eq. (7c) as

$$16 \quad F(\mathbf{S}'; \mathbf{S}) = \lim_{n' \rightarrow 0} \frac{1}{n'} \frac{dn'}{dt} = \lambda g(\mathbf{S}') - d(Y'), \quad (\text{E3a})$$

17 with  $g(\mathbf{S}')$  as specified in Eq. (D7) with

$$18 \quad \begin{aligned} \tilde{R}(\mathbf{S}') &= N(X', m_R, Y'^2 + \sigma_R^2), \\ \tilde{C}(\mathbf{S}') &= A \hat{n} N(X', X, Y'^2 + Y^2). \end{aligned} \quad (\text{E3b})$$

## 19 APPENDIX F: INVASION FITNESS IN THIRD MODEL

20 Here we derive the invasion-fitness function for the third model. First, the total resource dis-  
21 tribution is given by

$$22 \quad R(z) = B(z) + \sum_{j=1}^L n_j r(z, \mathbf{S}_j). \quad (\text{F1a})$$

1 The rate of actual resource gain by phenotype  $\mathbf{S}_i$  is then given by  $g(\mathbf{S}_i)$  as specified in Eq.  
 2 (D7) with

$$\begin{aligned}
 \tilde{R}(\mathbf{S}_i) &= \int c(z, \mathbf{S}_i) R(z) dz = R_0 N(X_i, m_R, \sigma_c^2 + \sigma_R^2) + \sum_{j=1}^L n_j N(X_i, Y_j, \sigma_c^2 + \sigma_r^2), \\
 \tilde{C}(\mathbf{S}_i) &= \int c(z, \mathbf{S}_i) C(z) dz = A \sum_{j=1}^L n_j N(X_i, X_j, \sigma_c^2),
 \end{aligned}
 \tag{F1b}$$

4 according to Eq. (D6), where  $C(z)$  is the total consumption effort invested on resource type  
 5  $z$  by all phenotypes  $\mathbf{S}_j$ , as given by Eq. (D2) By assuming that predators do not distinguish  
 6 phenotypes of prey when they share a same resource quality  $z$ , we obtain the functional  
 7 response of phenotype  $\mathbf{S}_i$  to  $\mathbf{S}_j$  as  $g(\mathbf{S}_i)$  multiplied by the fraction of  $\mathbf{S}_j$  in the re-  
 8 sources preyed upon by  $\mathbf{S}_i$ ,

$$g_p(\mathbf{S}_i, \mathbf{S}_j) = g(\mathbf{S}_i) \int c(z, \mathbf{S}_i) n_j r(z, \mathbf{S}_j) dz / \tilde{R}(\mathbf{S}_i) = g(\mathbf{S}_i) n_j N(X_i, Y_j, \sigma_c^2 + \sigma_r^2) / \tilde{R}(\mathbf{S}_i). \tag{F1c}$$

10 Second, the rate of biomass loss of phenotype  $\mathbf{S}_i$  per its unit biomass is then given by

$$l(\mathbf{S}_i) = \frac{1}{n_i} \sum_{j=1}^L n_j g_p(\mathbf{S}_j, \mathbf{S}_i) \tag{F2}$$

12 Third, for a monomorphic population with phenotype  $\mathbf{S}$  and equilibrium biomass  $\hat{n}$ , the  
 13 invasion fitness of a mutant phenotype  $\mathbf{S}'$  is then derived according to Eq. (8c) as

$$F(\mathbf{S}'; \mathbf{S}) = \lim_{n' \rightarrow 0} \frac{1}{n'} \frac{dn'}{dt} = \lambda g(\mathbf{S}') - g_p(\mathbf{S}, \mathbf{S}') - d, \tag{F3a}$$

15 with

$$\begin{aligned}
 \tilde{R}(\mathbf{S}') &= N(X', m_R, \sigma_c^2 + \sigma_R^2) + \hat{n} N(X', Y, \sigma_c^2 + \sigma_r^2), \\
 \tilde{C}(\mathbf{S}') &= A \hat{n} N(X', X, \sigma_c^2).
 \end{aligned}
 \tag{F3b}$$

Figure 1

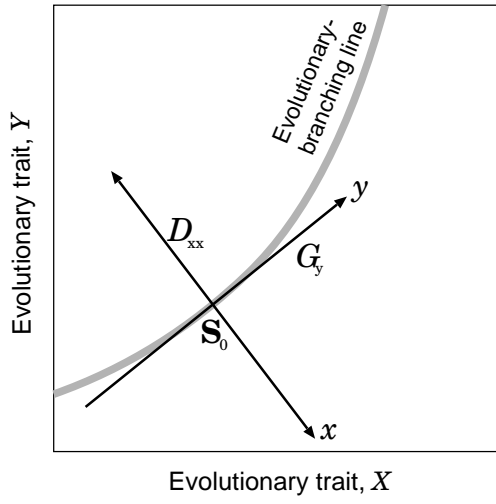


Figure 2

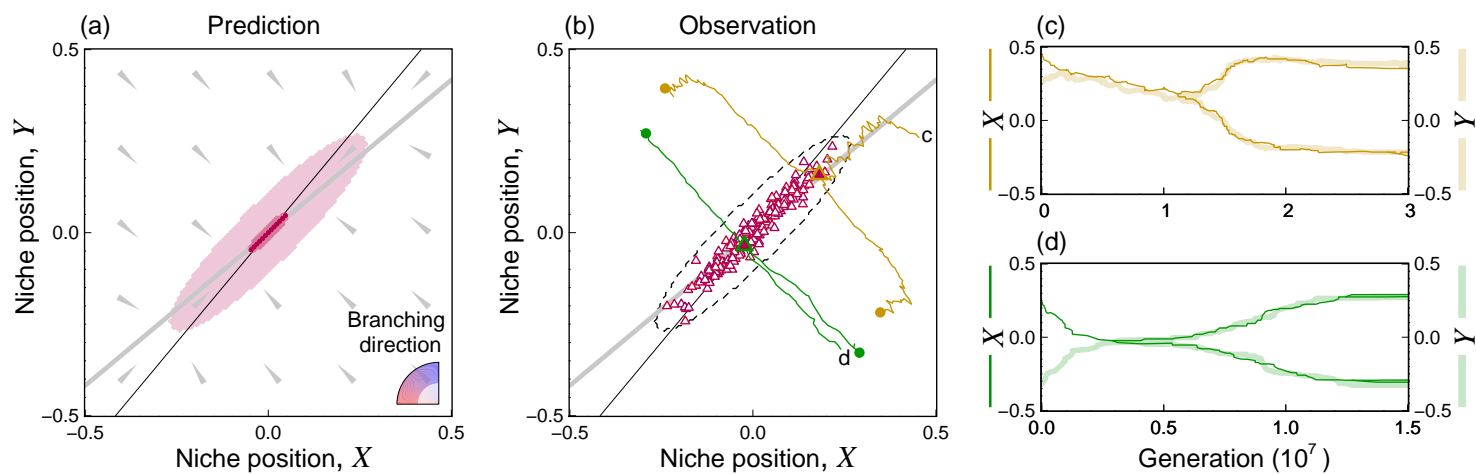


Figure 3

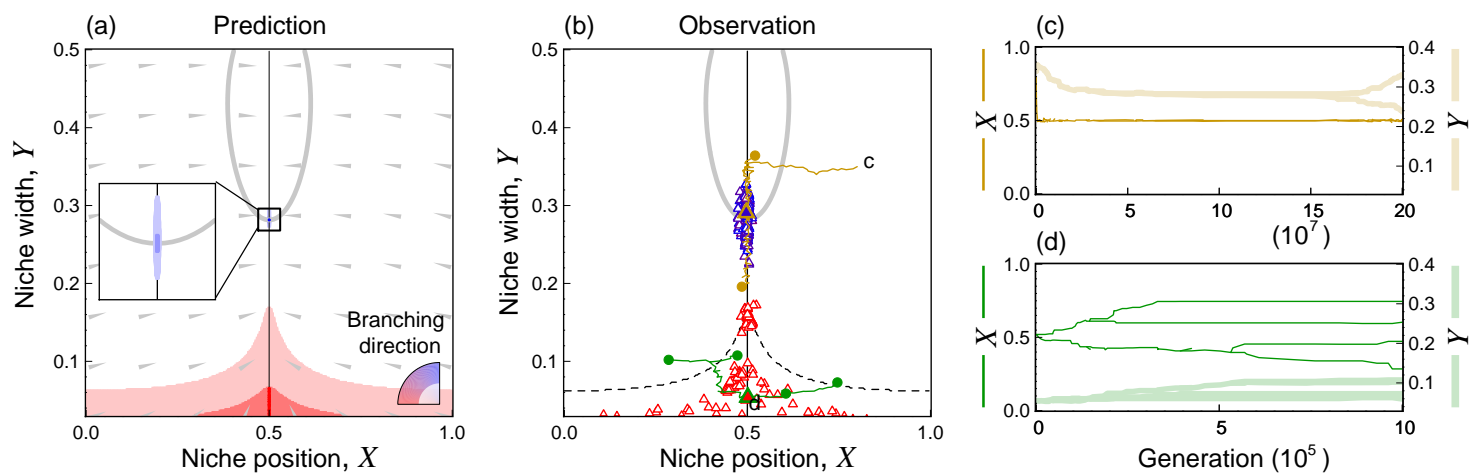


Figure 4

